

AD-A038 540

HARRY DIAMOND LABS ADELPHI MD  
A TENTATIVE MODEL OF THE SI-SIO2 INTERFACE.(U)  
FEB 77 M M SOKOŁOSKI  
HDL-TR-1787

F/G 9/1

UNCLASSIFIED

NL

| OF |  
AD  
A038 540



END  
DATE  
FILMED  
10-77  
DDC

HDL-TR-1787

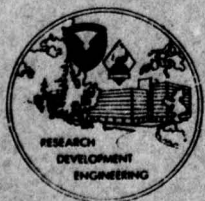
AD-A038540

TR-1787—A Tentative Model of the Si-SiO<sub>2</sub> Interface, by Martin M. Solzski

File Copy

# A Tentative Model of the Si-SiO<sub>2</sub> Interface

February 1977



U.S. Army Materiel Development  
and Readiness Command  
HARRY DIAMOND LABORATORIES  
Adelphi, Maryland 20783

Replacement copy of HDL-TR-1787

Previous copy obsolete; please destroy.

The findings in this report are not to be construed as an official Department of the Army position unless so designated by other authorized documents.

Citation of manufacturers' or trade names does not constitute an official indorsement or approval of the use thereof.

Destroy this report when it is no longer needed. Do not return it to the originator.

UNCLASSIFIED

SECURITY CLASSIFICATION OF THIS PAGE (When Data Entered)

REPORT DOCUMENTATION PAGE		READ INSTRUCTIONS BEFORE COMPLETING FORM
1. REPORT NUMBER HDL-TR-1787	2. GOVT ACCESSION NO.	3. RECIPIENT'S CATALOG NUMBER
4. TITLE (and Subtitle)  A Tentative Model of the Si-SiO <sub>2</sub> Interface		5. TYPE OF REPORT & PERIOD COVERED Technical Report
		6. PERFORMING ORG. REPORT NUMBER
7. AUTHOR(s)  Martin M. Sokoloski		8. CONTRACT OR GRANT NUMBER(s)  DA: 1T161102AH44
9. PERFORMING ORGANIZATION NAME AND ADDRESS Harry Diamond Laboratories 2800 Powder Mill Road Adelphi, MD 20783		10. PROGRAM ELEMENT, PROJECT, TASK AREA & WORK UNIT NUMBERS  Program Element: 6.11.02.A
11. CONTROLLING OFFICE NAME AND ADDRESS US Army Materiel Development & Readiness Command Alexandria, VA 22333		12. REPORT DATE February 1977
		13. NUMBER OF PAGES 49
14. MONITORING AGENCY NAME & ADDRESS (if different from Controlling Office)		15. SECURITY CLASS. (of this report)  Unclassified
		15a. DECLASSIFICATION/DOWNGRADING SCHEDULE
16. DISTRIBUTION STATEMENT (of this Report)  Approved for public release; distribution unlimited.		
17. DISTRIBUTION STATEMENT (of the abstract entered in Block 20, if different from Report)		
18. SUPPLEMENTARY NOTES  HDL Project: A44628 DRCMS Code: 611102.11.H4400		
19. KEY WORDS (Continue on reverse side if necessary and identify by block number)  Interface                      Band tails Heterojunction              Capacitance-voltage measurement Disorder                      Fluctuating interface potential		
20. ABSTRACT (Continue on reverse side if necessary and identify by block number)  A model of the electronic density of states in a metal-insulator-semiconductor structure is proposed. The model is based upon current theories of the electronic properties of amorphous materials and disordered alloys. The model accounts for the presence of "band-tail" states at the insulator-semiconductor interface and also speculates about the presence of states in the oxide as being due to persistent silicon conduction		

DD FORM 1473 1 JAN 73 EDITION OF 1 NOV 65 IS OBSOLETE

UNCLASSIFIED  
SECURITY CLASSIFICATION OF THIS PAGE (When Data Entered)

UNCLASSIFIED

SECURITY CLASSIFICATION OF THIS PAGE (When Data Entered)

and valence bands. The derivation of the admittance of a metal-oxide-semiconductor capacitor with a distribution of the interface states is reviewed, and an interpretation of these states employing the macroscopic theory of Brews is later derived. It is shown how these states can be measured by a quasi-static capacitance voltage measurement.

## CONTENTS

	<u>Page</u>
1. INTRODUCTION . . . . .	5
2. MICROSCOPIC THEORY . . . . .	11
2.1 Intrinsic Interface States . . . . .	11
2.2 Extrinsic Interface States . . . . .	20
3. FORMULATION . . . . .	21
3.1 Admittance for Distribution of Interface States . . . . .	21
3.2 Fluctuations in Potential . . . . .	29
3.3 Inclusion of Interface Potential Fluctuations on Admittance . . . . .	33
4. QUASI-STATIC CAPACITANCE VOLTAGE METHOD FOR MEASUREMENT OF DENSITY OF INTERFACE STATES . . . . .	38
4.1 Criteria for Reversibility . . . . .	38
4.2 Determination of Various Parameters in Density of States Formulation . . . . .	40
5. CONCLUSION . . . . .	42
LITERATURE CITED . . . . .	43
DISTRIBUTION . . . . .	45

## FIGURES

1 Metal-oxide-semiconductor capacitor . . . . .	5
2 An n-channel metal-oxide-semiconductor field-effect transistor . . . . .	6
3 One possible dependence of composition of graded A <sub>x</sub> B <sub>1-x</sub> heterojunction . . . . .	13

FIGURES (Cont'd)

	<u>Page</u>
4 Possible dependence of density of states for alloy $A B_x^{1-x}$ heterojunction . . . . .	14
5 Radial distribution curves for amorphous and crystalline Si as determined from analysis of electron diffraction data . . .	15
6 Metamorphosis of density of states from that in bulk $SiO_2$ to that in bulk Si . . . . .	17
7 Heterogeneous model . . . . .	18
8 Transition from glassy amorphous $SiO_2$ to crystalline Si state . . . . .	19
9 Circuit for metal-oxide-semiconductor capacitor with discrete noninteracting bound states in insulator-semiconductor interface . . . . .	27
10 Metal-oxide-semiconductor structure divided into two arbitrarily small areas of uniform charge density . . . . .	30
11 Oxide-semiconductor interface . . . . .	34

## 1. INTRODUCTION

Metal-insulator-semiconductor (MIS) structures and, in particular, those in which the insulator is an oxide of Si are being increasingly employed in both the civilian and military electronics markets. These structures are employed in a class of devices known as field effect transistors (FET's). When the FET consists of a metal-oxide-semiconductor (MOS) structure, it is then labeled MOSFET, or MOS device; insulated gate FET (IGFET) also occurs in the literature.

The MOS structure (fig. 1) is physically a semiconductor substrate (usually Si) on which is grown an oxide layer. Onto this is evaporated a thin metallic layer called the gate. The structure (sometimes called a MOS capacitor or diode) consists of a metal-insulator junction and an insulator-semiconductor junction. Since these junctions consist of two materials with a different band gap, they are called heterojunctions. In contrast, a p-n junction is a homojunction.

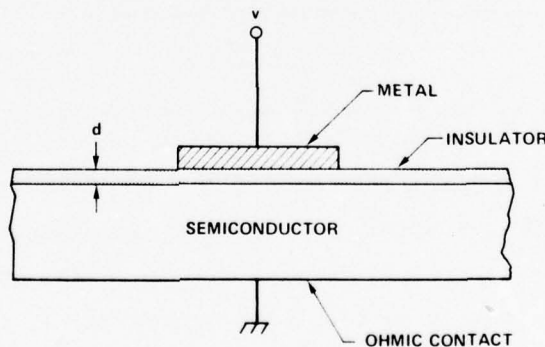


Figure 1. Metal-oxide-semiconductor capacitor.

The MOS structure is used mainly as a diagnostic tool to study phenomena associated with such heterojunctions. The actual useful device is the MOSFET (fig. 2). Before the oxide is grown on the

surface of the semiconductor substrate (p-type, fig. 2), two n+ regions called source and drain are diffused in the p-type bulk substrate (fig. 2). Ohmic contact is made to these, and a gate is then separated from the p-type bulk by an oxide layer. With no voltage on the gate, the current path from the source to the drain is effectively open. For the p-type bulk device, a positive voltage can be found whereby the electrons accumulate near the oxide-semiconductor interface and form a so-called inversion layer and short-circuit the source-drain electrodes. When a voltage difference is subsequently placed between the source and the drain, a current flows. The gate voltage at which this current flow begins is called the threshold voltage ( $V_T$ ).

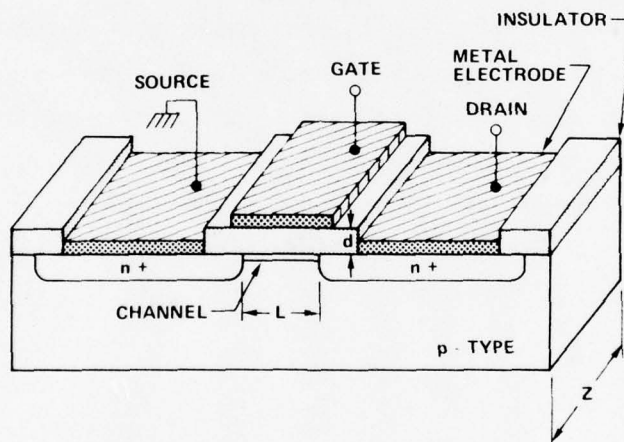


Figure 2. An n-channel metal-oxide-semiconductor field effect transistor.

There has been an extensive amount of experimental work on the nature of the oxide-semiconductor interface and, more specifically, the  $\text{SiO}_2$ -Si interface. The interface is composed, on one hand, of an amorphous insulator with a forbidden energy gap of approximately 8 to 9 eV and, on the other hand, of a semiconductor with a gap of approximately 1.1 eV at 300 K. At the interface, there are two types of electronic states: (1) those that are in the oxide and do not communicate with either the metal or semiconductor electrode and (2) those that are in the Si forbidden gap and do communicate with the semiconductor electrode.

There are other complications with this MOS system. For instance, depending on the history of the device, mobile ions (in particular,  $\text{Na}^+$ ) can exist in the oxide layer. With proper bias on the metal electrode and at elevated temperatures,\* the ions can be asymmetrically distributed with the mean of the distribution being near the metal oxide or near the oxide semiconductor interface.<sup>1</sup> In each instance, the ions form a dipole layer near the interface and cause a lowering of the interface barrier. Also, segregation of the impurity dopant atoms that were formerly in the bulk Si can occur in the oxide near the oxide-semiconductor interface. This occurrence, in turn, can either enhance or decrease the polarization layer due to the former mobile ions such as  $\text{Na}^+$ . In any case, such extrinsic impurities can affect the oxide-semiconductor interface and further complicate the physics of interface states. Hence, wherever possible, this discussion is on phenomena, experiments, and theories in which such extrinsic oxide ionic charges are negligible.

One can envision how the gross electronic properties of the oxide-semiconductor interface are manifested. One can imagine a perfect infinite semiconductor having a forbidden gap separating two bands of extended states called the valence and conduction bands. These states in which the carriers are characterized by a good quantum number (crystal momentum) are due to the long-range order in the crystalline semiconductor. However, to grow an oxide-semiconductor interface, one needs a surface. The introduction of a surface in the crystalline semiconductor breaks the long-range symmetry, with the subsequent result that electronic states localized near the surface can now exist in the gap. Carriers in these states cannot be characterized

---

<sup>1</sup>N. J. Chou, *J. Electrochem. Soc.*, 118 (1971), 601.

\*The elevated temperatures are used just to decrease the amount of time elapsed before a given amount of mobile ionic charge is transported to either interface.

by momentum alone since momentum is not a good quantum number. In Si, these states form two so-called surface bands centered slightly below and above the bulk conduction and valence bands. These bands were observed in work function and photoelectron threshold measurements on atomically clean Si surfaces.<sup>2</sup> Later, optical absorption due to transitions between these two bands was observed.<sup>3</sup> Electron paramagnetic resonance studies have established that the surface valence band consists of unpaired electrons.<sup>4</sup> Also, from photoemission studies, the surface valence band contains one electron per surface atom ( $8 \times 10^{14}$  electrons  $\text{cm}^{-2}$ ).<sup>5,6</sup> Theoretical calculations by Appelbaum and Hamann show a "single band" of gap states that are highly localized in the surface and have an unmistakable dangling bond shape.<sup>7</sup>

Hence, these localized surface band states represent an unnatural state. Upon exposure to the atmosphere, the atomically clean surface undergoes chemical reactions by saturating most dangling bonds and, thus, reduces the surface-free energy. This reduction takes place via the chemical absorption of a layer of  $\text{O}_2$ . The photoemission peak of the former surface valence band is practically eliminated.<sup>5</sup> What occurs is that the surface valence band and  $\text{O}_2$  p-orbitals form the oxide valence band below the Si band. Now as the Si surface is continually oxidized, some Si diffuses into the  $\text{SiO}_2$ , while, at the same time,  $\text{O}_2$  diffuses into the bulk Si. This is just another example of a system's lowering its free energy by the entropy of mixing. This process is continued in the manufacture of MOSFET devices until an oxide layer of approximately 100 nm is formed.

---

<sup>2</sup>F. G. Allen and G. W. Gobeli, *Phys. Rev.*, 127 (1962), 150.

<sup>3</sup>G. Cluarotti et al, *Phys. Rev.*, B4 (1971), 3398.

<sup>4</sup>D. Haneman, *Phys. Rev.*, 176 (1968), 705.

<sup>5</sup>L. F. Wagner and W. E. Spicer, *Phys. Rev. Lett.*, 28 (1972), 1381.

<sup>6</sup>D. E. Eastman and W. D. Grobman, *Phys. Rev. Lett.*, 28 (1972), 1378.

<sup>7</sup>J. A. Appelbaum and D. R. Hamann, *Phys. Rev. Lett.*, 31 (1973), 106.

We point out in section 2 that the interface should extend over several lattice spacings and should be very disordered. This disorder should give rise to fluctuations. In fact, in the course of their investigations on MOS-type devices, Nicollian and Goetzberger noticed a dispersion of interface-state time constants in the depletion region of gate voltage.<sup>8</sup>

At the same time, it was demonstrated both theoretically and experimentally that the strong surface electric field associated with a semiconductor inversion layer is sufficient to quantize motion of the charge carriers normal to the surface.<sup>9</sup> The levels in the inversion region consist of electric subbands, each of which is a two-dimensional Bloch state associated with one of the quantized levels. Indeed, these conclusions were corroborated by electron-tunneling, capacitance, and far-infrared cyclotron resonance studies of the quantized levels.<sup>10</sup>

It was suggested further that electrons in these inversion layers also behave like electrons in a two-dimensional disordered system, the disorder being due to the random fluctuating interface potential independently proposed by Nicollian and Goetzberger.<sup>8</sup> In other words, the random fluctuating potential should yield the characteristic temperature dependence of amorphous conductivity in the conductance channel,  $\sigma \propto T^{1/(d+1)}$  at low temperatures, where  $d$  is the dimensionality of the system.<sup>11</sup> Indeed, such a dependence of the low-temperature

---

<sup>8</sup>E. H. Nicollian and A. Goetzberger, *Bell Syst. Tech. J.*, 45 (1967), 1055.

<sup>9</sup>F. Stern and W. E. Howard, *Phys. Rev.*, 163 (1967), 816; A. B. Fowler, F. F. Fang, W. E. Howard, and P. J. Stiles, *Phys. Rev. Lett.*, 16 (1966), 901.

<sup>10</sup>D. C. Tsui, *Phys. Rev.*, B4 (1971), 4438; *Phys. Rev.*, B8 (1973), 2657; S. James Allen, D. C. Tsui, and J. V. Dalton, *Phys. Rev. Lett.*, 32 (1974), 107; D. C. Tsui, G. Kaminsky, and P. H. Schmidt, *Phys. Rev.*, B9 (1974), 3524.

<sup>11</sup>R. Am Abram, *J. Phys. Chem.*, 6 (1973), L379; V. D. S. Shante, *Phys. Lett.*, 43A (1973), 249.

channel conductance has been recently seen and reported.<sup>12</sup> The fluctuating potential at the interface is necessary to explain the behavior of the inversion layer carrier mobility as a function of carrier concentration and temperature.<sup>13</sup> Finally, measurements of the resonant absorption of photons due to transitions between the quantized levels show a distortion of the resonance line width that can be caused by a fluctuating surface potential.<sup>14,15</sup>

Hence, these independent measurements strongly indicate that the surface potential at an oxide-semiconductor interface is not a smooth function, but is more akin to a random fluctuating potential somewhat similar to that observed in amorphous solids. We theorize that these fluctuations are the result of the loss of long-range order as the Si is "alloyed" with the oxide. This alloying tends to cause band-tail states extending into the gap in both the Si valence and conduction bands. These states we call "intrinsic" interface states, since they arise from the inherent disorder introduced by the alloying. Also, in the oxide are localized states that cannot communicate with the semiconductor, metal electrodes, or both. These states are notorious hole traps. We speculate that any holes trapped in these states increase the fluctuations and, in turn, increase the band-tail states or interface states. Such a theory accounts for the U-shaped, structureless, measured density of states curves.<sup>14</sup> It accounts also for an approximately equal number of electron and hole states. On the other hand, models that depend on an isolated microscopic defect to account for the interface states are hard pressed to explain all the characteristics of the measured density of states.

---

<sup>12</sup>H. Ibach and J. E. Rowe, *Phys. Rev.*, B9 (1974), 1951.

<sup>13</sup>A. G. Revesz et al, *J. Phys. Chem. Solids*, 28 (1967), 197.

<sup>14</sup>R. Castagne and A. Vapaille, *Electronic Letters*, 6 (1970), 691.

<sup>15</sup>M. Kuhn and E. H. Nicollian, *J. Electrochem. Soc.*, 118 (1971), 370.

In section 3, we review the derivation of the admittance of an MOS capacitor with a distribution of localized states. Then we indicate how one can interpret these interface potential fluctuations via a macroscopic theory of Brews.<sup>16</sup> These interface states can be measured by a variety of techniques, one of which we have specifically considered--the quasi-static capacitance voltage measurement (QSCV).<sup>17</sup> We also indicate the necessary conditions of reversibility that must be satisfied in order to use the QSCV technique.

## 2. MICROSCOPIC THEORY

### 2.1 Intrinsic Interface States

The MOS system is quite complicated. The first complication is that the system is heterogeneous--that is, the properties of the system are origin dependent. Also, the electronic properties range from extended conduction in the metal to phonon-assisted tunneling through band-tail states in the oxide. Nonetheless, we should like to speculate using the knowledge of the physics of ordered and disordered systems on the properties at and near the oxide-semiconductor interface.

Ion backscatter studies indicate that this region is not sharp.<sup>18</sup> Instead, the oxide appears to be stoichiometric up to the interface while having an ever increasing concentration of Si. This is to be physically expected from the entropy of mixing. During the

---

<sup>16</sup>J. R. Brews, *J. Appl. Phys.*, 43 (1972), 2306; 3451.

<sup>17</sup>C. N. Berglund, *IEEE Trans. Electron Devices*, ED-13 (1966), 701; M. Kuhn, *Solid-State Electron.*, 13 (1970), 873.

<sup>18</sup>W. K. Chu, E. Lugujo, and J. W. Mayer, *Appl. Phys. Lett.*, 24 (1974), 105.

growth process, two materials, the Si and oxide thereof, are present and in contact at high temperatures. The total system at this elevated temperature can reduce its free energy by increasing the entropy due to mixing. Therefore, one should expect a large concentration of Si in the oxide at the interface. On the other hand, the Si being used to grow the oxide is already saturated with a large concentration of  $O_2$ , since the Si crystals used in MOSFET devices are pulled from quartz crucibles.\* Therefore rather than being a sharp mathematical plane separating two nonmixed solid phases, the interface appears to be more of an alloyed heterojunction--the excess Si and  $O_2$  concentrations persisting into the oxide and semiconductor regions, respectively. The adage that nature abhors a singularity is the rule in this case. Nevertheless, a description of the junction as a "gradual heterojunction" is indeed simplified. Not only does the junction undergo a compositional gradient, but long-range order disappears, and the nearest-neighbor lattice constant changes. These physical changes, needless to say, have severe ramifications on the electrical properties of the system and, in particular, at the oxide-semiconductor junction.

One approach to the problem of an oxide-semiconductor junction is to investigate the nature of the density of states in a gradual gap heterojunction. Unfortunately, this problem has yet to be solved. However, it can be qualitatively modeled by an alloy in which the composition,  $x$ , is a function of direction. The subsequent alloy,  $A_x B_{1-x}$ , can then closely model a graded heterojunction by the appropriate choice of the spatial composition dependence as indicated in figure 3 for a Fermi type of compositional dependence,

$$x = [\exp(-\beta z) + 1]^{-1}.$$

---

\*At the melt temperature, there is an equilibrium distribution of dissolved  $O_2$  in Si. Most  $O_2$  remains in the Si crystal structure as bound interstitial impurities. The interaction of this interstitial  $O_2$  with a lattice vacancy gives rise to the infamous Si-A center with an electron trapping level 0.17 eV below the conduction band.

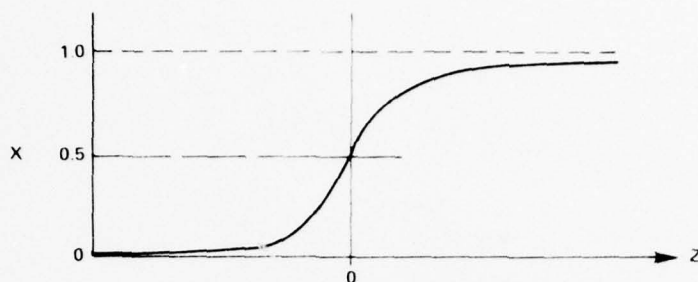


Figure 3. One possible dependence of composition of graded  $A_xB_{1-x}$  heterojunction.

Here,  $\beta$  is a measure of the amount of mixing, the "effective" junction width being just twice the inverse of  $\beta$ . From our knowledge of the alloy density of states for homogeneous materials,<sup>19</sup> we can say that the density of states of a graded heterojunction should behave somewhat similarly to that in figure 4.<sup>20</sup> For simplicity, only one band has been shown. In the model,  $\epsilon_A$  and  $\epsilon_B$  are the mean band positions. As the concentration of the A species increases, an impurity band forms in which the states are purely localized as the hatched marks indicate (see fig. 4). This localized A band grows with increasing distance into the junction until, at  $z = 0$ , there are equal compositions of A and B. Then as the B species decreases, the A band becomes more and more extended until, at large distances, the material consists of all A atoms. This highly idealized picture serves two purposes: (1) the density of states is position dependent, and (2) there will exist *localized* states in and around the junction.

In our actual oxide-Si interface, the details are more complicated. The lattice constant changes, and the oxide is disordered (lacks long-range order). In the binary alloy model of a heterojunction, there is a basic lattice; the disorder originates in

<sup>19</sup>P. Soven, *Phys. Rev.*, 156 (1967), 809; B. Velicky, S. Kirkpatrick, and H. Ehrenreich, *Phys. Rev.*, 175 (1968), 746.

<sup>20</sup>M. M. Sokoloski, *Bull. Am. Phys. Soc.*, 20 (1975), 426.

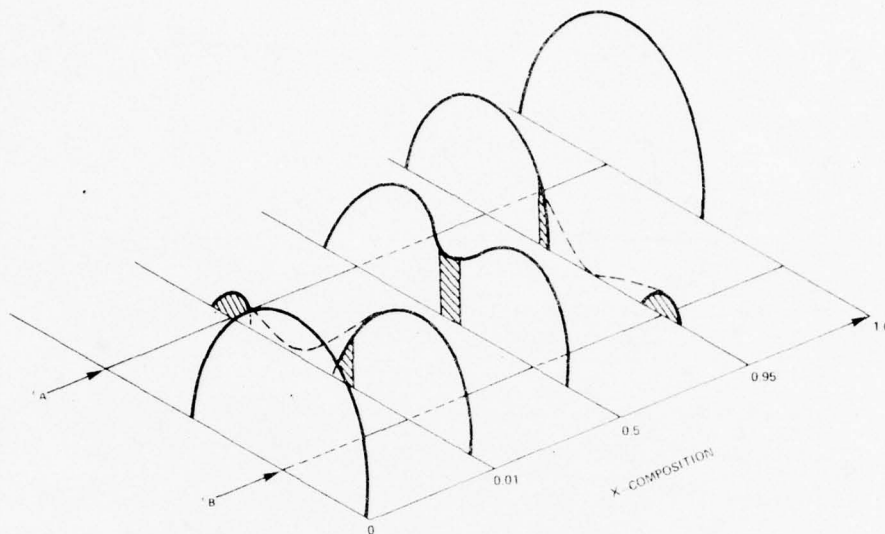


Figure 4. Possible dependence of density of states for alloy  $A_xB_{1-x}$  heterojunction:  $x$  has position dependence of fig. 3; point  $x = 0$  corresponds to pure B material  $z = -\infty$ ; while for  $x = 1$ ,  $z = +\infty$ . For  $x = 0.5$ ,  $z = 0$ , the middle of the heterojunction.

the random placement of A and B atoms on the lattice. This type of disorder is called compositional disorder. In the oxide-semiconductor case, there is also topological disorder. Here the oxide is not unlike that of an amorphous solid where the binding forces between the atoms are still similar to those in a crystal, but long-range order is absent while short-range order of a few lattice constants are generally present.<sup>21</sup> From the angular dependence of the scattered radiation of an x-ray diffraction pattern, the radial or pair distribution function  $4\pi r^2 \rho(r) dr$  can be obtained through a Fourier inversion. This yields the number of pairs of atoms separated by a distance lying between  $r$  and  $r + dr$ . As an example, the experimental radial distribution curves (RDC's) for amorphous and crystalline Si are shown in figure 5.<sup>22</sup> If

<sup>21</sup>N. F. Mott and E. A. Davis, *Electronic Processes in Non-Crystalline Materials*, Clarendon Press, Oxford, England (1971).

<sup>22</sup>S. C. Moss and J. F. Graczk, *Phys. Rev. Lett.*, 23 (1969), 1167; S. C. Moss and J. F. Graczk, *Proceedings of the 10th International Conference on the Physics of Semiconductors*, Cambridge, MA (1970), 658.

the peaks in the RDC are well separated from adjacent ones, then the area beneath the first peak, for instance, yields the number of atoms in the first coordination sphere; i.e., the first nearest neighbors in a crystal lie on the periphery of a sphere.

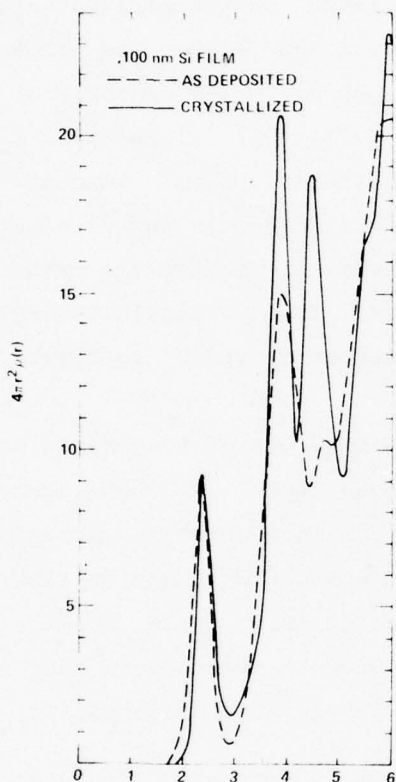


Figure 5. Radial distribution curves for amorphous and crystalline Si as determined from analysis of electron diffraction data.

is loss of long-range order. This loss implies also that charge carriers can no longer be specified by a good quantum number of crystalline momentum. In actuality, the carrier's mobility is now a function of its energy.

For both the amorphous and crystalline states of Si, the first peak is at an interatomic spacing of 0.235 nm and has a coordination number of 4. Each atom is separated from four nearest neighbors by the lattice constant of 0.235 nm. The second peak is the same for both crystalline and amorphous Si with a spacing of 0.386 nm and coordination number of 12. However, the third peak present in the crystalline state is dramatically absent in the amorphous curve. This absence means that given a particular site, we no longer can predict with certainty the position of the third nearest neighbor atom. There

Because of the loss of long-range order and associated fluctuations in matrix elements, the oxide gap cannot be described by the wide gap of an insulator. Electrons that make transitions out of the valence states into the conduction states do not necessarily leave behind holes with definite momentum or enter extended states. The loss of long-range order and presence of associated potential fluctuations lead to the possibility of extended and localized states as shown in figure 6. Now the density of states does not go to zero sharply at the valence or conduction band edge, but tails off. These band tails consist of localized states, i.e., states that conduct by phonon-assisted tunneling. Above a certain energy in the conduction band and below that in the valence band, the states are extended; transport can be considered as crystalline. This particular energy is known as the mobility edge and is designated as  $E_c$  and  $E_v$  in figure 7.

However, we have been discussing the loss of long-range order and potential fluctuations in homogeneous systems. In heterogeneous systems, the radial distribution function must now be origin dependent. For instance, if one examines the radial distribution function (RDF) in the bulk of the Si in our MOS-structure, one would obtain the crystalline RDC's. In contrast, if the RDF were examined in the oxide bulk, one would obtain RDC's similar to those of amorphous, glassy  $\text{SiO}_2$ .

The oxide-semiconductor junction is not sharp. Also, there is a loss of long-range order and an associated increase in potential fluctuations as the origin is moved from the bulk Si to the oxide-semiconductor interface. Therefore, the interface should be characterized, in part, by a region of localized states that lie in the semiconductor gap. These states, indicated by the hatched areas in figures 4 and 6, would then be a manifestation of the loss of long-range order and an increase in potential fluctuations. These states would

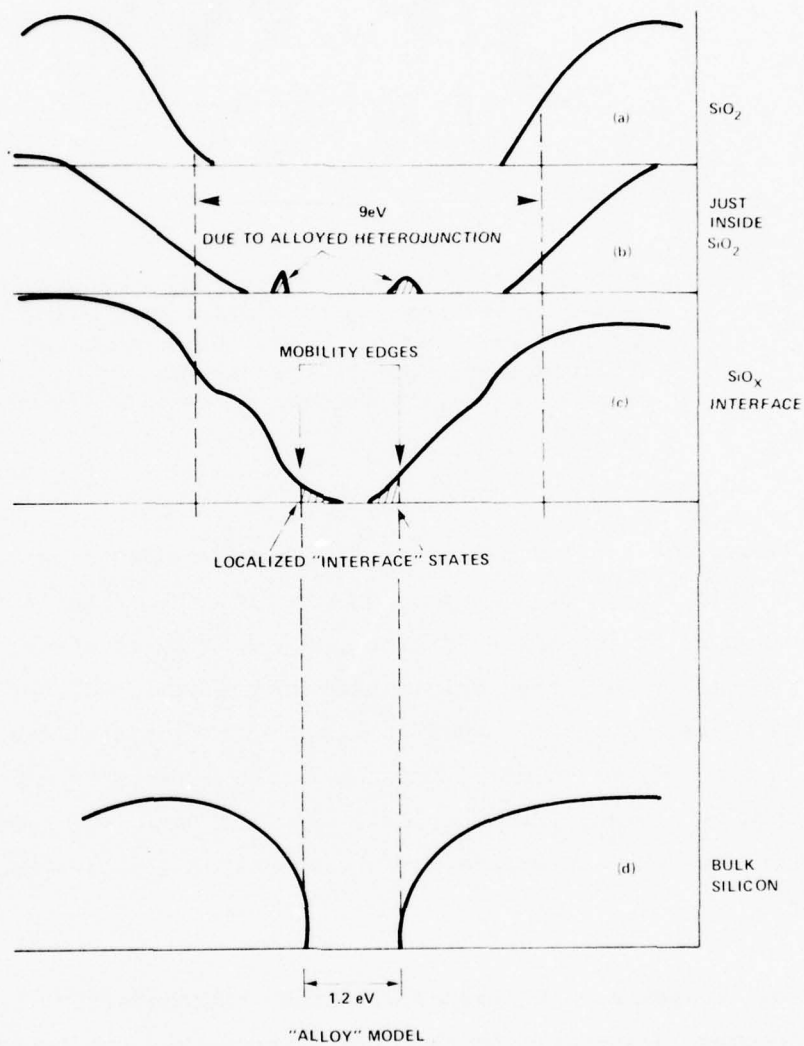


Figure 6. Metamorphosis of density of states from that in bulk  $\text{SiO}_2$  (a) to that in bulk Si (d).

then be intrinsic interface states. Their sole claim to existence would be due to the glassy amorphous  $\text{SiO}_2$  to crystalline Si transition, and they should occur in all such systems.

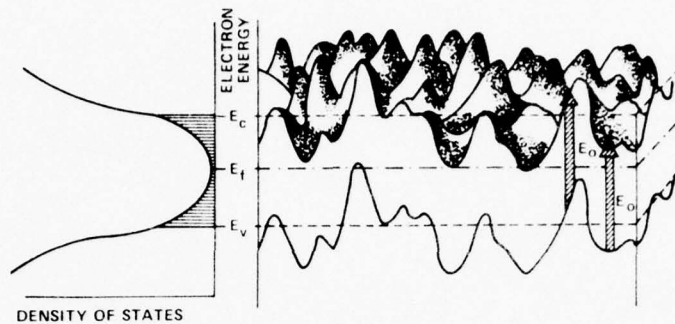


Figure 7. Heterogeneous model: right-hand side shows edges of valence and conduction bands modified by long-wavelength electrostatic potential fluctuations; optical transitions take place with energy  $E_0$ ; localized states lie between  $E_c$  and  $E_0$ .

Hence, one can formulate the following argument: As the origin is moved from the bulk semiconductor in the direction of the oxide-semiconductor interface (fig. 6), the density of states undergoes a metamorphosis. For the origin deep in the semiconductor bulk, the density of states is just equal to that of the crystalline material. The RDF is that of the ordered material. The effects of the interface are screened out by any free carriers. As the origin is moved closer and closer to the interface, the effects of disorder become more important.

For instance, in figure 8, the tetrahedrally coordinated lattice becomes disordered as the origin approaches the interface. At sites labeled 2 and 3, the number of semiconductor atoms in the first coordination sphere begins to differ from that in the bulk semiconductor. Close to the interface, this loss of long-range order

introduces localized states in the Si energy gap as indicated in figure 6. These localized states are in "communication" with the bulk semiconductor; i.e., there can be transport in and out of these states to the bulk semiconductor valence and conduction bands.

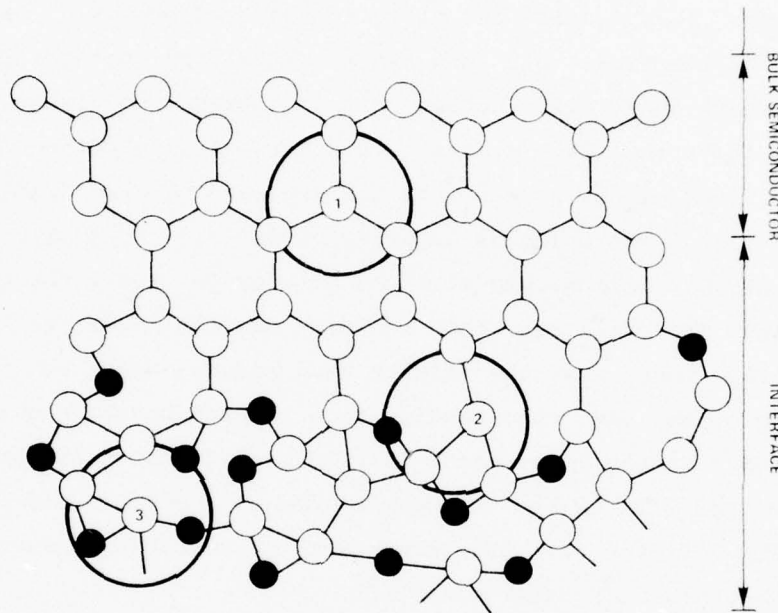


Figure 8. Transition from glassy amorphous  $\text{SiO}_2$  to crystalline Si state.

There is an approximately equal number of these states above and below the intrinsic Fermi level as can be seen from figure 7. This U-shape for the localized states, more popularly known as interface states, has been seen experimentally by a whole host of independent experimenters.<sup>14,23</sup>

Previous theories of these states have accounted for the shape of the interface-state density curves as being due to a particular defect at the interface. However, it is exceedingly difficult to justify that

<sup>14</sup>R. Castagne and A. Vapaille, *Electronic Letters*, 6 (1970), 691.

<sup>23</sup>R. Castagne and A. Vapaille, *Surface Science*, 28 (1971), 157; *Electron. Lett.* 6 (1970), 691; D. J. Silversmith, *J. Electrochem. Soc.*, 119 (1972), 1589.

this level spreads across the gap (for Si, energies exceed 1 eV) because a level splits as a result of interactions with the immediate environment. Also, it is difficult to make isolated defect trap holes and then electrons depending on the position of the Fermi level. Therefore, the result of alloying the semiconductor with its oxide introduces the loss of long-range order and potential fluctuations. These result in a distribution of localized gap states referred to as band tails or interface states. In tetrahedrally bonded semiconductors, because of alloying, remnants of the s-p bonding and antibonding bands persist into the oxide as impurity bands (fig. 4, 6(b)). These states may or may not communicate with the bulk oxide; i.e., the phonon-assisted tunneling probabilities may be very small. Some of these states, especially those near the valence band edges, may be responsible for trapping holes and thus leading to a trapped positive charge density in the oxide. On the other hand, it is expected that transport in the oxide can be modeled by the continuous-time-random-walk model of Scher and Montroll modified by an imperfectly absorbing boundary at the oxide-semiconductor interface.<sup>24, 25</sup>

## 2.2 Extrinsic Interface States

Experimentally, it is well known that oxide charge is trapped close to the interface and ordinarily cannot tunnel into the bulk semiconductor. This trapping may result from a persistent impurity band extending into the oxide due to the incomplete alloying at the interface (a preponderance of Si atoms, for instance). The trapping should give rise to an electrostatic potential. However, because of the inherent disorder in the interface, this charge and its resultant

<sup>24</sup>H. Scher and E. W. Montroll, *Phys. Rev.*, B12 (1975), 2455; H. E. Boesch, F. B. McLean, J. M. McGarrity, and G. A. Ausman, Jr., *IEEE Trans. Nucl. Sci.*, NS-22 (1975), 2163.

<sup>25</sup>F. B. McLean, G. A. Ausman, H. E. Boesch, J. M. McGarrity, J. *Appl. Phys.*, 47 (1976), 1529.

potential are not uniform, but fluctuate about some mean. These fluctuations, in turn, produce further fluctuations that cause the bands to vary as schematically indicated in figure 7. Hence, these potential fluctuations (as compared to potential fluctuations due to matrix elements fluctuating about some mean value) also lead to trapping states and band tails. Therefore, the interface-state density also is a function of the amount of charge trapped in the oxide; i.e., the more charge trapped in the oxide, the greater the potential fluctuations and the more the interface-state density.

One can then define those states due to potential fluctuations from a trapped oxide charge distribution as being "extrinsic." Therefore, the overall microscopic picture is that the intrinsic interface states are inherently due to the loss of long-range order due to the nature of the oxide-semiconductor heterojunction. Also, charges trapped in localized oxide states, which may be due to remanant s-p bonding and antibonding states of the semiconductor, can cause an increase in the density of interface states, and these new states are extrinsic. Extrinsic states are due also to impurities and defects at the interface not accounted for in the heterojunction model.

### 3. FORMULATION

#### 3.1 Admittance for Distribution of Interface States

The admittance of a distribution of localized states in the semiconductor forbidden gap and fluctuations in the interface potential can be derived by (1) calculating the admittance of a single localized level via Shockley-Read statistics,<sup>26</sup> (2) averaging over a density of localized states, and (3) averaging over fluctuations in interface potential.<sup>8</sup>

<sup>8</sup>E. H. Nicollian and A. Goetzberger, *Bell Syst. Tech. J.*, 45 (1967), 1055.

<sup>26</sup>W. Shockley and W. T. Read, *Phys. Rev.*, 87 (1952), 835.

States that occur in the gap are bound states. The capture rate of electrons taken as the majority carrier at some energy is then

$$R_n(t) = N_s c_n [1 - f(t)] n_s(t), \quad (1)$$

while the emission rate is

$$G_n(t) = N_s e_n f(t), \quad (2a)$$

where  $N_s$  is the density of bound interface states per  $\text{cm}^{-2}$ ,  $c_n$  is the electron capture probability in  $\text{cm}^3/\text{s}$ ,  $e_n$  is the electron emission constant in  $\text{s}^{-1}$ ,  $f(t)$  is the Fermi distribution at time  $t$ , and  $n_s(t)$  is the electron density at the localized trap site at time  $t$  in  $\text{cm}^{-3}$ . This is a special case in which the density of interface states (in  $\text{cm}^{-2} \text{eV}^{-1}$ ) is given by

$$N_{ss}(\psi) = N_s \delta(\psi - \psi_t),$$

where  $\psi_t$  is the energy of the bound state. Since electrons are being trapped, the bound states at the interface are either negatively charged (the state is filled) or neutral (the state is unoccupied). Such an interface state is sometimes called an acceptor surface state. Then the trap occupation probability

$$f_o(t) = [1 + \exp(\psi_t - \psi_F(t))/kT]^{-1} = [1 + \exp(\psi_t - \psi_B + \psi_s(t))/kT]^{-1} \quad (2b)$$

where  $\psi_F(t)$  is the Fermi level,  $\psi_B$  is the bulk Fermi level, and  $\psi_s$  is the surface potential. In equation (1), the capture rate depends on the occupancy of the bound state, i.e.,  $N_s(1 - f(t))$ , and the number of electrons,  $n(t)$ , that are available to make a transition to this bound state. On the other hand, the transition from a bound state to the conduction-band continuum is independent of the final-state Fermi

function only in depletion. Hence, equation (2a) is a good approximation, except in heavy inversion or accumulation. The net current flowing equals the electronic charge,  $q$ , multiplying the difference of the capture and emission rates, namely,

$$i_s(t) = qN_s c_n [1 - f(t)] n_s(t) - qe_n N_s f(t) . \quad (3)$$

For no external alternating stimulus,  $i_s(\text{dc}) = 0$ . This is sometimes referred to as detailed balancing. Equation (3) can be solved in a linear approximation by expanding all time-dependent variables,  $x(t)$ , in a Taylor series expansion about their static values,

$$\begin{aligned} x(t) &= x_0 + \left. \frac{\partial x}{\partial t} \right|_0 \delta t + \dots \\ &= x_0 + \delta x . \end{aligned} \quad (4)$$

These are substituted into the current equation, i.e.,

$$\begin{aligned} i_s(t) &= qN_s c_n \left[ (1 - f_0) n_{s0} + (1 - f_0) \delta n_s - n_{s0} \delta f \right] \\ &\quad - qe_n N_s (f_0 + \delta f) , \end{aligned} \quad (5)$$

where second-order terms have been neglected. Equation (5) can be manipulated so that

$$\begin{aligned} qN_s c_n (1 - f_0) n_{s0} - qe_n N_s f_0 &= i_s(t) - qN_s c_n \left[ (1 - f_0) \delta n_s - n_{s0} \delta f \right] \\ &\quad + qe_n N_s \delta f . \end{aligned} \quad (6)$$

The left-hand side is independent of the time and, thus, is a constant. From detail balancing, this constant is set equal to zero. Statically, no net current flows--a particle emitted from the bound state is then captured. This places a constraint on the emission rate, namely,

$$e_n = c_n n_{s0} (1 - f_0) / f_0 . \quad (7)$$

This can be substituted into the right-hand side of equation (6), and an expression for the current is obtained:

$$\begin{aligned} i_s(t) &= qN_s c_n \left[ (1 - f_o) \delta n_s - n_{so} \frac{\delta f}{f} \right] \\ &= qN_{ss} \frac{df}{dt} . \end{aligned} \quad (8)$$

Hence, for an applied field with frequency  $\omega$ ,

$$\begin{aligned} \frac{df}{dt} &= i\omega \delta f \\ &= c_n (1 - f_o) \delta n_s - c_n n_{so} \frac{\delta f}{f} . \end{aligned} \quad (9)$$

This can be subsequently solved for  $\delta f$ .

$$\begin{aligned} \delta f &= \frac{f_o c_n (1 - f_o) \delta n_s}{c_n n_{so} + i\omega f_o} \\ &= \frac{f_o (1 - f_o)}{1 + i\omega f_o / c_n n_{so}} \frac{\delta n_{so}}{n_{so}} . \end{aligned} \quad (10)$$

The substitution of equations (9) and (10) into equation (8) yields

$$i_s(t) = \frac{i\omega q N_s f_o (1 - f_o)}{1 + i\omega f_o / c_n n_{so}} \frac{\delta n_{so}}{n_{so}} . \quad (11)$$

From

$$n_s = n_i \exp(u_s - u_B) , \quad (12)$$

it can be shown that

$$\begin{aligned} \delta n_s &= n_i \exp(u_s - u_B) \delta u_s \\ &= n_s \delta u_s , \end{aligned} \quad (13)$$

where  $u_s$  and  $u_B$  are the interface and bulk potentials in units of  $kT/q$  and  $n_i$  is the intrinsic carrier density.<sup>8</sup> Therefore,

$$\frac{\delta n_s}{n_{so}} = \delta u_s \quad (14)$$

$$= q/kT \times \delta \psi_s, \quad (15)$$

where  $\psi_s$  is the interface potential in electron volts. Therefore, the substitution of equation (14) into equation (11) finally yields an expression for the admittance of a single bound state  $N_s$ , i.e.,

$$i_s(\omega) = Y_s(\omega) \delta \psi_s, \quad (16)$$

where

$$Y_s(\omega) = i\omega \frac{q^2 N_s f_o (1 - f_o)}{kT (1 + i\omega f_o / c n_{so})}. \quad (17)$$

Now if one calls

$$C_{ss}^0 \equiv q^2 N_s f_o (1 - f_o) / kT \quad (18)$$

and defines a majority carrier time constant

$$\tau \equiv f_o / c n_{so}, \quad (19)$$

then one can write

$$Y_s(\omega) = G_p(\omega) + i\omega C_p(\omega), \quad (20)$$

where the equivalent capacitance and parallel conductance are given as

$$C_p = \frac{C_{ss}^0}{1 + \omega^2 \tau^2} \quad (21)$$

<sup>8</sup>E. H. Nicollian and A. Goetzberger, *Bell Syst. Tech. J.*, 45 (1967), 1055.

and

$$G_P = \frac{C_{SS}^0 \omega^2 \tau^2}{1 + \omega^2 \tau^2} . \quad (22)$$

The dc or static limit of the equivalent capacitance is just  $C_{SS}^0$ . Also,  $f^0(1 - f^0)$  is sharply peaked with spread  $kT$  about the bound state energy,  $\psi_t$ . There,  $C_{SS}^0$  has its maximum value when  $\psi_t = \psi_f$ . For the MOS capacitor, this equivalent capacitance appears in parallel with the space-charge capacitance, shown as follows.

The total charge density for a given interface potential is

$$Q_T = Q_{SC} + Q_S + Q_f , \quad (23)$$

where  $Q_{SC}$  is the charge in the Si-space-charge region,  $Q_S$  is the charge in the interface (bound) states, and  $Q_f$  is the charge in the fixed states. The charge in the fixed states, as the name implies, cannot communicate with either the metal or the semiconductor electrodes. "Communicate" means to make a quantum mechanical transition via some process such as tunneling or phonon-assisted hopping from the bound-state site (in the oxide) to either the metal or the semiconductor. The total current is then the time rate of change of the total charge,

$$i_S(t) = \frac{dQ_{SC}}{dt} + \frac{dQ_S}{dt} \quad (24a)$$

$$= \frac{dQ_{SC}}{d\psi_S} \frac{d\psi_S}{dt} + i_S(t) , \quad (24b)$$

$$i_S(t) = (i\omega C_P + Y_S) \delta\psi_S . \quad (24c)$$

Equation (24c) is derived partly from the substitution of equation (16) for the bound-state current and the realization that

$$C_{sc} = dQ_{sc} / d\psi_s \quad \text{and} \quad \psi_s = \psi_{so} + \delta\psi_{so}$$

$$\text{where } \delta\psi_{so} = a \exp(i\omega t) .$$

Hence, equation (24c) shows that the bound-state admittance appears in parallel with the capacitance of the semiconductor space-charge layer. Figure 9 shows the equivalent circuit for the MOS capacitor with discrete noninteracting bound states that are physically in the oxide-semiconductor region.

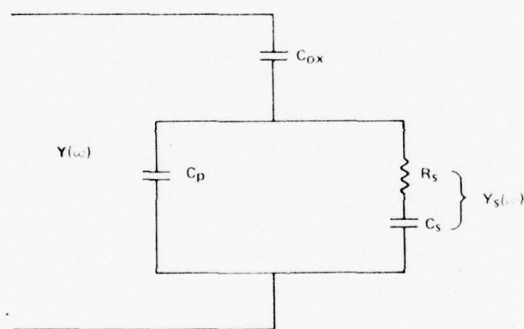


Figure 9. Circuit for metal-oxide-semiconductor capacitor with discrete noninteracting bound states in insulator-semiconductor interface.

The admittance due to a number of noninteracting bound states is given by equation (17). This can be easily extended to a distribution of localized-interface states by integrating over the potential, since  $N_{ss}$  is now a function of potential, i.e.,

$$Y_{ss}(\omega) = i\omega \left( \frac{q^2}{kT} \right) \int \frac{N_{ss}(\psi) f_o (1 - f_o) d\psi}{1 + i\omega f_o / c_n n_{so}} \quad (25)$$

where  $N_{ss}(\psi)$  is the density of states and  $\psi$  is energy.<sup>25</sup> The Fermi distribution is now a continuous function of potential (i.e.,  $\psi_t$  is now a continuum of values,  $\psi$ ).

For a density-of-states function and a capture cross section that do not change appreciably within  $kT$  of  $\psi_f$ , the distribution,  $N_{ss}(\psi)$ , can be taken out of the integral and evaluated at  $\psi_f = \psi_s - \psi_B$ , and the capture cross section can be treated as constant. Then one can make the substitution that

$$df_o/d\psi = -q/kT \times f_o(1 - f_o)$$

and transform equation (25) into an integral over  $f_o$  with lower and upper boundaries of 0 and 1, respectively. The integrand is separated into real and imaginary parts,

$$\int = \int_0^1 \frac{df_o}{1 + f_o^2 \omega^2 \tau^2} - i\omega\tau \int_0^1 \frac{f_o df_o}{1 + f_o^2 \omega^2 \tau^2} \quad (26a)$$

This can be readily integrated to yield

$$Y_{ss} = \frac{qN_{ss}}{2\tau} \ln(1 + \omega^2 \tau^2) + iq \frac{N_{ss}}{\tau} \tan^{-1}(\omega\tau) \quad (26b)$$

The corresponding conductance and admittance are given by

$$G_{ss}(\psi_s) = \frac{qN_{ss}(\psi_s)}{2\tau} \ln(1 + \omega^2 \tau^2) \quad (27a)$$

and

$$C_{ss}(\psi_s) = qN_{ss}(\psi_s) \frac{1}{\omega\tau} \tan^{-1}(\omega\tau) \quad (27b)$$

<sup>25</sup>F. B. McLean, G. A. Ausman, H. E. Boesch, J. M. McGarrity, J. Appl. Phys., 47 (1976), 1529.

Equations (27a) and (27b) yield the proper static equation  $\omega = 0$ ; in particular, the static capacitance due to a distribution of surface states is

$$C_{SS}(\psi_s) = qN_{SS}(\psi_s) . \quad (28)$$

This equation could have been derived in a more straightforward manner by integrating the expression for the dc or static capacitance for the case of (noninteracting) isolated bound states,

$$C_{SS}(\psi_s) = \int C_{SS}^0(\psi) d\psi \quad (29a)$$

$$= \int q^2 N_{SS}(\psi) f_o(1 - f_o) / kT d\psi , \quad (29b)$$

in which  $N_{SS}(\psi)$  does not vary much over energy.

### 3.2 Fluctuations in Potential

To treat the problem of fluctuating interface potentials, we shall employ the phenomenological approach of Nicollian and Goetzberger<sup>8</sup> as extended by Brews.<sup>16</sup> According to Brews,<sup>16</sup> the interface charge due to any trapped oxide charge and charge trapped in the Si-band-tail states near the interface can be treated by a distribution of uncorrelated characteristic areas,  $\alpha$ , each with a charge density as shown in figure 10. Each characteristic area varies in properties from other areas according to some probability distribution. For each of the characteristic areas, one can write

$$(\psi_g - \psi_s) C_{ox}^\alpha = Q^\alpha + Q_{sc}^\alpha(\psi_s) , \quad (30)$$

<sup>8</sup>E. H. Nicollian and A. Goetzberger, *Bell Syst. Tech. J.*, 45 (1967), 1055.

<sup>16</sup>J. R. Brews, *J. Appl. Phys.*, 43 (1972), 2306; 3451.

where  $\psi_g$  and  $\psi_s$  are the gate and surface potentials, respectively, of the  $\alpha$ th area. Also,  $C_{ox}^\alpha$ ,  $Q^\alpha$ , and  $Q_{sc}^\alpha$  are the oxide capacitance, charge, and space charge associated with area  $\alpha$ . According to Brews,<sup>16</sup> a similar expression is assumed to be valid for the entire macroscopic structure,

$$(\psi_g - \bar{\psi}_s)C_{ox} = \bar{Q} + \bar{Q}_{sc}(\psi_s) . \quad (31)$$

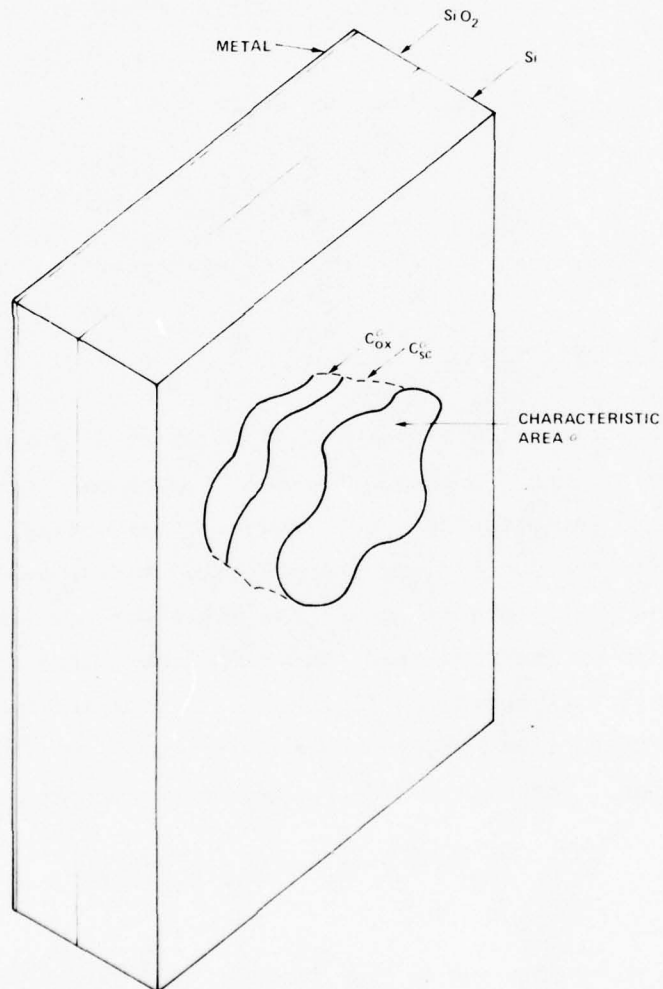


Figure 10. Metal-oxide-semiconductor structure divided into two arbitrarily small areas of uniform charge density.

<sup>16</sup>J. R. Brews, *J. Appl. Phys.*, **43** (1972), 2306; 3451.

The bars indicate that the quantities that are statistically varying over the macroscopic structure have been suitably averaged. What we really seek is the average of not the macroscopic structure, but the  $\alpha$ th area. It can be found by dividing equation (31) by  $N = (\alpha/A)^{-1}$ , where  $N$  is the number of macroscopic areas, while  $A$  is the total area of the macroscopic structure. Then equation (31) becomes

$$(\psi_g - \bar{\psi}_s) C_{ox}^\alpha = \bar{Q}^\alpha + \overline{Q_{sc}^\alpha(\psi_s)} . \quad (32)$$

In the Brews<sup>8,16</sup> approach,  $C_{ox}$  is statistically a constant. The bars with superscript  $\alpha$ 's indicate averages of the parameters describing the  $\alpha$ th area.

The derivations of the true values must be found about their average values. Hence, equation (32) is subtracted from equation (31) to yield

$$(\psi_s - \bar{\psi}_s) C_{ox}^\alpha = Q^{s'} - \bar{Q}^\alpha + \left[ \overline{Q_{sc}^\alpha(\psi_s)} - \overline{Q_{sc}^\alpha(\bar{\psi}_s)} \right] . \quad (33)$$

Unfortunately, the space charge is a nonlinear function of the surface potential. However, for small surface potential fluctuations, the average space charge can be linearized as follows:

$$\overline{Q_{sc}^\alpha(\psi_s)} \approx \bar{\psi}_s C_{sc}^\alpha(\bar{\psi}_s) . \quad (34)$$

<sup>8</sup>E. H. Nicollian and A. Goetzberger, *Bell Syst. Tech. J.*, 45 (1967), 1055.

<sup>16</sup>J. R. Brews, *J. Appl. Phys.*, 43 (1972), 2306; 3451.

The total charge on each area consists of fixed charges that are not in communication with either the metal or the semiconductor electrode or charges in states that are mobile, i.e., interface states,

$$Q^\alpha - \overline{Q^\alpha} = Q_f^\alpha - \overline{Q_f^\alpha} + Q_{ss}^\alpha - \overline{Q_{ss}^\alpha} .$$

A crucial assumption of Brews<sup>16</sup> is that since the interface charge,  $Q_{ss}^\alpha$ , is mobile, these charges, on one hand, tend to screen out potential fluctuations and, on the other hand, tend to increase the potential fluctuations by trapping additional charges. Hence, this assumption can be modeled in a quasi-self-consistent manner by decomposing the interface charge into two components,

$$Q_{ss}^\alpha - \overline{Q_{ss}^\alpha} = C_{ss}^\alpha (\psi_s - \overline{\psi_s}) + \delta Q_{ss}^\alpha , \quad (36)$$

where the first term accounts for the screening and the last accounts for inhomogeneities. Then, following Brews,<sup>16</sup> we define the variation in fixed charge by

$$\delta Q_f^\alpha \equiv Q_f^\alpha - \overline{Q_f^\alpha} \quad (37)$$

and find that the variation in total interface charge can be written as

$$\delta Q^\alpha \equiv \delta Q_f^\alpha + \delta Q_{ss}^\alpha . \quad (38)$$

By the substitution of equations (33) to (37) into equation (38), one finally obtains the variations (fluctuations) in the interface charge in terms of the variations (fluctuations) in the surface potential as

$$\delta Q^\alpha = \left[ C_{ox}^\alpha + C_{ss}^\alpha (\overline{\psi_s}) + C_{sc}^\alpha (\overline{\psi_s}) \right] \delta \psi_s . \quad (39)$$

---

<sup>16</sup>J. R. Brews, *J. Appl. Phys.*, 43 (1972), 2306; 3451.

Hence,

$$\overline{(\delta\psi_s)^2} = \left[ C_{ox}^\alpha + C_{ss}^\alpha(\psi_s) + C_{sc}^\alpha(\psi_s) \right]^{-2} (\delta Q^\alpha)^2 . \quad (40)$$

However,

$$\overline{(\delta Q^\alpha)^2} = \overline{(\delta Q_f^\alpha)^2} + \overline{(\delta Q_{ss}^\alpha)^2} + 2 \overline{(\delta Q_f^\alpha)(\delta Q_s^\alpha)} . \quad (41)$$

In the approach of Nicollian and Goetzberger,<sup>8</sup> the last cross term in equation (41) is neglected, since the two charge distributions are considered uncorrelated, and the term  $C_{ss}^\alpha(\bar{\psi}_s)$  is absent in equation (40). If one defines capacitance per unit area by dividing by  $\alpha$ , i.e.,  $C_{ox} = \alpha^{-1} C_{ox}^\alpha$ , then

$$\sigma(\bar{\psi}_s) = \frac{W(\bar{\psi}_s)}{W(\bar{\psi}_s) [C_{ox} + C_{ss}(\bar{\psi}_s)] + \epsilon_{si}} \left( \frac{qQ}{\alpha} \right)^2 \quad (42)$$

where  $W(\bar{\psi}_s)$  is the space charge width shown in figure 11,  $\epsilon_{si}$  is the dielectric constant of Si, and  $q$  is the electronic charge. As is pointed out by Brews,<sup>16</sup> a large  $C_{ss}$  leads to a smaller  $\sigma^2$ , which is a result of the screening effect.

### 3.3 Inclusion of Interface Potential Fluctuations on Admittance

From accumulation to flat band, the majority carriers in the semiconductors tend to screen and damp out fluctuations in the interface potential as can be seen from equation (42). However, from flat band to depletion, the screening effect is drastically decreased while more image charge appears in the metal electrode and causes fluctuations. The effects of the fluctuations should increase with increasing depletion width saturating at inversion. In contrast,

<sup>8</sup>E. H. Nicollian and A. Goetzberger, *Bell Syst. Tech. J.*, **45** (1967), 1055.

<sup>16</sup>J. R. Brews, *J. Appl. Phys.*, **43** (1972), 2306; 3451.

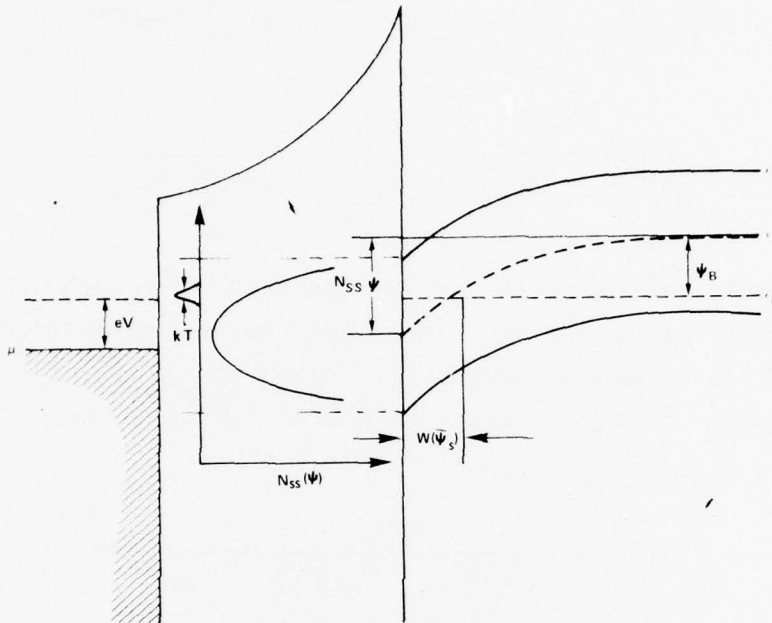


Figure 11. Oxide-semiconductor interface.

surface states oppose any increases in interface potential fluctuations by filling and unfilling, to compensate for variations in the mean trapped and interface charges. The zero frequency (quasi-static) surface-state capacitance averaged over the fluctuations in the interface potential is given by

$$\overline{C_{SS}(\psi)} = \frac{C_M(\psi)C_{OX}}{C_{OX} - C_M(\psi)} - \overline{C_{SC}(\psi)}, \quad (43)$$

where  $C_M(\psi)$  is the measured value of the capacitance,  $C_{OX}$  is the geometric capacitance of the oxide layer, and  $\overline{C_{SC}}$  is the average space-charging capacitance. The static or zero frequency average surface-state capacitance can be written as

$$\overline{C_{SS}(\psi_S)} = \int qN_{SS}(\psi) P(\psi, \bar{\psi}_S) d\psi_S, \quad (44)$$

where the kernel is given as

$$P(\psi, \bar{\psi}_S) = (2\pi\sigma^2)^{-1/2} \exp \left[ -(\psi - \bar{\psi}_S)^2 / \sigma(\bar{\psi}_S) \right]. \quad (45)$$

Hence,  $N_{SS}(\psi)$  is the density of interface-states function being nonzero only for  $\bar{\psi}_S$  falling in the energy interval between the Si conduction and valence bands. It is also a positive definite compact function whose area yields the total number of interface states. The variance,  $\sigma(\bar{\psi}_S)$ , is given by equation (42). For a p-type semiconductor, the space-charge width is given approximately by

$$W(\bar{\psi}_B) = 0, \quad \bar{\psi}_S < \psi_{FB} \quad (46a)$$

$$= \left( \frac{2\epsilon_{Si}\bar{\psi}_S}{qN_A} \right)^{1/2} \psi_{FB} \leq \bar{\psi}_S \leq \psi_{INV} \quad (46b)$$

$$= \left( \frac{2\epsilon_{Si}\psi_{INV}}{qN_A} \right)^{1/2} \psi_{INV} \leq \bar{\psi}_S, \quad (46c)$$

where  $\psi_{FB}$  is the flat-band potential,  $N_A$  is the acceptor density, and  $\psi_{INV}$  is the inversion value of the interface potential,

$$\psi_{INV} = \frac{2kT}{q} \ln \left( N_A / n_i \right), \quad (47)$$

where  $n_i$  is the intrinsic carrier concentration at temperature  $T$ . Therefore, the functional dependence of all quantities on the surface potential is known. Hence, in accumulation, where most of the carriers are heavily screening the interface potential fluctuations, the space charge width is approximately zero. In this region, the fluctuations are ineffective, i.e.,

$$P(\psi, \bar{\psi}_S) = \delta(\psi - \bar{\psi}_S), \quad (48)$$

where  $\delta(\psi - \bar{\psi}_s)$  is the dirac delta function. From flat band to inversion, the variance becomes a monotonically increasing function of space-charge width. The bar is dropped from  $\bar{\psi}_s$  for notational simplicity.

The corresponding damping effect of the fluctuating potential by the surface states manifests itself in the dependence of the variance on the true surface-state capacitance, i.e.,

$$C_{ss}(\psi) = qN_{ss}(\psi) . \quad (49)$$

To determine  $N_{ss}(\psi)$ , the basic equation to be solved is

$$C_p(\psi_s) = \frac{C_M(\psi_s)C_{ox}}{C_{ox} - C_M(\psi_s)} \quad (50)$$

$$= \int_{\psi_v}^{\psi_c} [qN_{ss}(\psi) - C_{sc}(\psi)] P(\psi, \psi_s) d\psi , \quad (51)$$

where  $\psi_c$  and  $\psi_v$  are the interface potentials at the conduction and valence band edges, respectively. Equation (51) must be solved self-consistently, since  $P(\psi, \psi_s)$ , in turn, is a function of  $N_{ss}(\psi)$ .  $C_p(\psi_s)$  is the parallel capacitance value of the surface state and space-charge capacitance. The gap,  $\psi_c - \psi_v$ , is divided into  $N$  parts of equal width,  $\Delta\psi$ . Then the first order in  $\Delta\psi$ , equation (51), can be written as

$$C_p(\psi_s) = \sum_{i,j=1}^{N+1} [qN_{ss}(\psi_i) - C_{ss}(\psi_i)] P(\psi_i, \psi_s) \Delta\psi , \quad (52)$$

where

$$\psi_1 = \psi_v \quad \text{and} \quad \psi_{N+1} = \psi_c .$$

Also,  $\psi_s$  can be divided into  $N$  units. Then

$$C_p(\psi_{sj}) = \sum_{i,j=1}^{N+1} [q_{ss}^N(\psi_i) - C_{sc}(\psi_i)] P(\psi_i, \psi_{sj}) \Delta\psi . \quad (53)$$

Then one can define the following  $N$ -fold vectors

$$C_p \equiv \frac{1}{\Delta\psi} [C_p(\psi_{sj})] , \quad (54a)$$

$$qN_{ss} = [q_{ss}^N(\psi_i)] , \quad (54b)$$

$$C_{ss} = [C_{ss}(\psi_i)] , \quad (54c)$$

and the square matrix

$$P = [P(\psi_i, \psi_{sj})] . \quad (55)$$

Then equation (52) can be simply written as

$$C_p = [qN_{ss} - C_{sc}] P(N_{ss}) , \quad (56)$$

where the dependence of  $P$  on  $N_{ss}$  has been shown. For  $P$  nonsingular, one can write

$$qN_{ss} = P(N_{ss})^{-1} C_p + C_{sc} . \quad (57)$$

If one defines the initial value  $N_{ss}^0 \equiv \langle N_{ss} \rangle$  as the average measured value, then one can iteratively solve for  $N_{ss}$ , i.e.,

$$qN_{ss}^{i+1} = P^{-1}(N_{ss}^i)^{-1} C_p + C_{sc} . \quad (58)$$

#### 4. QUASI-STATIC CAPACITANCE VOLTAGE METHOD FOR MEASUREMENT OF DENSITY OF INTERFACE STATES

##### 4.1 Criteria for Reversibility

Three common experimental techniques are used to determine the density of interface states at a heterojunction such as that found in an MOS capacitor. These are the Gray-Brown,<sup>27</sup> Nicollian-Goetzberger,<sup>8</sup> and QSCV<sup>28</sup> techniques.

In the Gray-Brown technique,<sup>27</sup> the variation in the charge density bound in the interface states is measured after the bulk Fermi level is displaced by a temperature change in the device. The Gray-Brown technique has been shown to be invalid at large interface-state densities, e.g.,  $10^{13} \text{ cm}^2 (\text{eV})^{-1}$ .<sup>29</sup> These temperature-dependent techniques and variations thereof give rise to a peak in the density of interface states near each of the Si conduction and valence band edges. These peaks are highly suspect, since they have not been seen by any other experimental technique.

In the Nicollian-Goetzberger<sup>8</sup> conductance technique, the measurements are limited in the accumulation end of the range, because the capture cross section is difficult to measure, and the interface density of the states is rapidly varying over several  $kT$ . Hence, the density of interface states is obtained in a limited region bound by the value of the surface potential corresponding to mid gap and flat band.

<sup>8</sup>E. H. Nicollian and A. Goetzberger, *Bell Syst. Tech. J.*, 45 (1967), 1055.

<sup>27</sup>P. V. Gray and D. M. Brown, *Appl. Phys. Lett.*, 8 (1966), 31; D. M. Brown and P. V. Gray, *J. Electrochem. Soc.*, 115 (1968), 760.

<sup>28</sup>G. Dedherck, R. Van Overstraeten, and G. Brown, *Solid-State Electron.*, 16 (1973), 1451.

<sup>29</sup>H. A. Mar and J. Simon, *Solid-State Electron.*, 17 (1974), 131.

<sup>30</sup>M. Kuhn, *Solid-State Electron.*, 13 (1970), 873.

In the QSCV technique,<sup>28</sup> the interface potential is varied so that the system is always at equilibrium. Small errors in the integration constant have a great influence on the density of states value in accumulation and strong inversion. Nevertheless, it is superior to low frequency capacitance-voltage techniques when the minority carrier lifetimes are large, since in these instances, the generation recombination times are very small.<sup>30</sup>

The advantage in the use of the QSCV technique<sup>28</sup> is that the system at all times is at thermodynamic equilibrium. Hence, the capacitance of the MOS system is just the oxide capacitance in series with a parallel combination of the average space-charge and interface-state capacitances for each value of the interface potential (gate potential) as given by equation (43). In other words, parameters dependent on the charge-carrier lifetimes and appearing as resistive components are zero for a static measurement. The QSCV technique involves sweeping the interface potential,  $\psi_s$ , at a certain rate. The criteria for thermodynamic reversibility, closely following the work of Kuhn,<sup>30</sup> is that

$$\tau_j (d\psi_B/dt) \leq kT/q, \quad (59)$$

for  $j$  corresponding to either electrons or holes. The lifetime  $\tau_j$  is given by

$$\tau_j = (\bar{v}\sigma_j n_i)^{-1} \exp \left[ \frac{q(\psi_B - \psi_s)}{kT} \right], \quad (60)$$

where  $\bar{v}$  is the average drift velocity and  $\sigma_j$  is the capture cross section due to the interface states for either electrons or holes.

<sup>28</sup>G. Dedherck, R. Van Overstraeten, and G. Brown, *Solid-State Electron.*, 16 (1973), 1451.

<sup>30</sup>M. Kuhn, *Solid-State Electron.*, 13 (1970), 873.

Hence, equation (59) states that the interface potential sweep rate must be such that the carriers making transitions in and out of the interface states can follow the changing potential at temperature  $T$ . If so, then the system at this sweep rate is always in equilibrium. In addition, in inversion, the sweep rate must be less than the minority-carrier generation rate. However, in the QSCV technique, the longest time constant is about  $10^{-2}$  s at room temperature, which is much smaller than the minority-carrier generation rate in inversion. Hence, the sweep rate need only maintain the inversion layer in equilibrium with the bulk semiconductor. The criterion is then given, for the positive bulk, as

$$\Delta F \approx \left( \frac{N_A V_D}{2q\epsilon_{si}} \right)^{1/2} \frac{\tau_0}{n_i} C_{ox} \frac{dV}{dt}, \quad (61)$$

where  $\Delta F$  is the difference between the surface quasi- and bulk Fermi level,  $V_D$  is the effective diffusion potential,  $\tau_0$  is the bulk minority-carrier lifetime, and  $V$  is the gate voltage.

#### 4.2 Determination of Various Parameters in Density of States Formulation

To calculate the density of states, various needed quantities can be systematically obtained. For instance, from values of the measured capacitance at infinite frequencies,  $C_m^{(\infty)}$ , the maximum depletion width can be found,

$$W = \left[ \frac{C_{ox} - C_M^{(\infty)}}{C_{ox} C_M^{(\infty)}} \right] \epsilon_{si}. \quad (62)$$

Then, for instance, for positive-bulk semiconductors, the doping density,  $N_A$ , can be determined via

$$N_A^{-1} \ln (N_A/n_i) = \frac{q^2 W}{4\epsilon_{si} kT} \cdot \quad (63)$$

Given this, one can easily determine the bulk potential,  $\psi_B$ , i.e.,

$$\psi_B = \frac{kT}{q} \ln N_A \cdot \quad (64)$$

Then one can determine the one-to-one functional dependence between the actual external potential,  $V$ , and the interface potential via Berglund's formula,

$$\psi(V) - \psi_B = \int_{V_{FB}}^V \left[ 1 - \frac{C_M(\zeta)}{C_{OX}} \right] d\zeta, \quad (65)$$

where the flat-band voltage,  $V_{FB}$ , can be obtained from the formula

$$C_{FB}(V_{FB}) = C_{OX} \left[ 1 - \frac{1}{\sqrt{2}} \left( \frac{C_{OX}}{\epsilon_{si}} \right) L \right]^{-1}, \quad (66)$$

where the Debye length,  $L$ , is given by

$$L = \left( \frac{2\epsilon_{si} kT}{q^2 p_0} \right)^{1/2} \cdot \quad (67)$$

At the same time, the mean average charge, which is needed in equation (42) for the variance, can be obtained from the flat-band voltage, i.e.,

$$V_{FB} = \phi_{ms} - \bar{Q}_{OX}^{-1}, \quad (68)$$

where  $\phi_{ms}$  is the metal-semiconductor work function.

## 5. CONCLUSION

States associated with the oxide-semiconductor consist of two types, intrinsic and extrinsic. The intrinsic states are manifestations of the heterogeneous nature of the interface, i.e., the loss of both topological and compositional disorder. The extrinsic states, on the other hand, arise due to fluctuations in the interface potential and impurities. This equipotential surface cannot be treated as a flat sheet.

The incorporation of both types of states into a phenomenological treatment based on that of Nicollian and Goetzberger<sup>8</sup> and Brews<sup>16</sup> will enable one to self-consistently calculate the true density of interface states (without the effects of fluctuations).

---

<sup>8</sup>E. H. Nicollian and A. Goetzberger, *Bell Syst. Tech. J.*, 45 (1967), 1055.

<sup>16</sup>J. R. Brews, *J. Appl. Phys.*, 43 (1972), 2306; 3451.

LITERATURE CITED

- (1) N. J. Chou, J. Electrochem. Soc., 118 (1971), 601.
- (2) F. G. Allen and G. W. Gobeli, Phys. Rev., 127 (1962), 150.
- (3) G. Cluarotti et al, Phys. Rev., B4 (1971), 3398.
- (4) D. Haneman, Phys. Rev., 176 (1968), 705.
- (5) L. F. Wagner and W. E. Spicer, Phys. Rev. Lett., 28 (1972), 1381.
- (6) D. E. Eastman and W. D. Grobman, Phys. Rev. Lett., 28 (1972), 1378.
- (7) J. A. Appelbaum and D. R. Hamann, Phys. Rev. Lett, 31 (1973), 106.
- (8) E. H. Nicollian and A. Goetzberger, Bell Syst. Tech. J., 45 (1967), 1055.
- (9) F. Stern and W. E. Howard, Phys. Rev., 163 (1967), 816; A. B. Fowler, F. F. Fang, W. E. Howard, and P. J. Stiles, Phys. Rev. Lett., 16 (1966), 901.
- (10) D. C. Tsui, Phys. Rev., B4 (1971), 4438; Phys. Rev., B8 (1973), 2657; S. James Allen, D. C. Tsui, and J. V. Dalton, Phys. Rev. Lett., 32 (1974), 107; D. C. Tsui, G. Kaminsky, and P. H. Schmidt, Phys. Rev., B9 (1974), 3524.
- (11) R. Am Abram, J. Phys. Chem., 6 (1973), L379; V. D. S. Shante, Phys. Lett., 43A (1973), 249.
- (12) H. Ibach and J. E. Rowe, Phys. Rev., B9 (1974), 1951.
- (13) A. G. Revesz et al, J. Phys. Chem. Solids, 28 (1967), 197.
- (14) R. Castagne and A. Vapaille, Electronic Letters, 6 (1970), 691.
- (15) M. Kuhn and E. H. Nicollian, J. Electrochem. Soc., 118 (1971), 370.
- (16) J. R. Brews, J. Appl. Phys., 43 (1972), 2306; 3451.
- (17) C. N. Berglund, IEEE Trans. Electron Devices, ED-13 (1966), 701; M. Kuhn, Solid-State Electron., 13 (1970), 873.

LITERATURE CITED (Cont'd)

- (18) W. K. Chu, E. Lugujo, and J. W. Mayer, *Appl. Phys. Lett.*, 24 (1974), 105.
- (19) P. Soven, *Phys. Rev.*, 156 (1967), 809; B. Velicky, S. Kirkpatrick, and H. Ehrenreich, *Phys. Rev.*, 175 (1968), 746.
- (20) M. M. Sokoloski, *Bull. Am. Phys. Soc.*, 20 (1975), 426.
- (21) N. F. Mott and E. A. Davis, *Electronic Processes in Non-Crystalline Materials*, Clarendon Press, Oxford, England (1971).
- (22) S. C. Moss and J. F. Graczk, *Phys. Rev. Lett.*, 23 (1969), 1167; S. C. Moss and J. F. Graczk, *Proceedings of the 10th International Conference on the Physics of Semiconductors*, Cambridge, MA (1970), 658.
- (23) R. Castagne and A. Vapaille, *Surface Science*, 28 (1971), 157; *Electron. Lett.* 6 (1970), 691; D. J. Silversmith, *J. Electrochem. Soc.*, 119 (1972), 1589.
- (24) H. Scher and E. W. Montroll, *Phys. Rev.*, B12 (1975), 2455; H. E. Boesch, F. B. McLean, J. M. McGarrity, and G. A. Ausman, Jr., *IEEE Trans. Nucl. Sci.*, NS-22 (1975), 2163.
- (25) F. B. McLean, G. A. Ausman, H. E. Boesch, J. M. McGarrity, *J. Appl. Phys.*, 47 (1976), 1529.
- (26) W. Shockley and W. T. Read, *Phys. Rev.*, 87 (1952), 835.
- (27) P. V. Gray and D. M. Brown, *Appl. Phys. Lett.*, 8 (1966), 31; D. M. Brown and P. V. Gray, *J. Electrochem. Soc.*, 115 (1968), 760.
- (28) G. Dedherck, R. Van Overstraeten, and G. Brown, *Solid-State Electron.*, 16 (1973), 1451.
- (29) H. A. Mar and J. Simon, *Solid-State Electron.*, 17 (1974), 131.
- (30) M. Kuhn, *Solid-State Electron.*, 13 (1970), 873.

DISTRIBUTION

COMMANDER  
US ARMY MATERIEL DEVELOPMENT  
& READINESS COMMAND  
500 EISENHOWER AVENUE  
ALEXANDRIA, VA 22333  
ATTN DRXAM-TL, HQ TECH LIBRARY

COMMANDER  
USA RSCH & STD GP (EUR)  
BOX 65  
FPO NEW YORK 09510  
ATTN LTC JAMES M. KENNEDY, JR.  
CHIEF, PHYSICS & MATH BRANCH

COMMANDER  
USA ARMAMENTS COMMAND  
ROCK ISLAND, IL 61201  
ATTN AMSAR-ASF, FUZE DIV  
ATTN AMSAR-RDF, SYS DEV DIV - FUZES

COMMANDER  
USA MISSILE & MUNITIONS CENTER & SCHOOL  
REDSTONE ARSENAL, AL 35809  
ATTN ATSK-CTD-F

DIRECTOR  
DEFENSE COMMUNICATIONS AGENCY  
WASHINGTON, DC 20305  
ATTN CODE 930, MONTE I. BURGETT, JR

DEFENSE DOCUMENTATION CENTER  
CAMERON STATION  
ALEXANDRIA, VA 22314  
ATTN TC-TCA, (12 COPIES)

DIRECTOR  
DEFENSE INTELLIGENCE AGENCY  
WASHINGTON, DC 20301  
ATTN DS-4A2

DIRECTOR  
DEFENSE NUCLEAR AGENCY  
WASHINGTON, DC 20305  
ATTN DDST  
ATTN RAEV  
ATTN STTL TECH LIBRARY  
ATTN STVL  
ATTN RATN

ENERGY RESEARCH & DEVELOPMENT AGENCY  
MATERIALS RADIATION EFFECTS BR  
DIV OF CONTROLLED THERMONUCLEAR FUSION  
WASHINGTON, DC 20545  
ATTN MARVIN COHEN

COMMANDER  
FIELD COMMAND  
DEFENSE NUCLEAR AGENCY  
KIRTLAND AFB, NM 87115  
ATTN FCPR

DIRECTOR  
INTERSERVICE NUCLEAR WEAPONS SCHOOL  
KIRTLAND AFB, NM 87115  
ATTN DOCUMENT CONTROL

DIRECTOR  
JOINT STRATEGIC TARGET  
PLANNING STAFF, JCS  
OFFUTT AFB  
OMAHA, NB 68113  
ATTN JLTW-2

CHIEF  
LIVERMORE DIVISION, FIELD COMMAND DNA  
LAWRENCE LIVERMORE LABORATORY  
P.O. BOX 808  
LIVERMORE, CA 94550  
ATTN DOCUMENT CONTROL FOR L-395  
ATTN FCPR

DIRECTOR  
NATIONAL SECURITY AGENCY  
FT. GEORGE G. MEADE, MD 20755  
ATTN O. O. VAN GUNTEN-R-425  
ATTN TDL

PROJECT MANAGER  
ARMY TACTICAL DATA SYSTEMS  
US ARMY ELECTRONICS COMMAND  
FORT MONMOUTH, NJ 07703  
ATTN DRCPN-TDS-SD  
ATTN DWAIN B. HUEWE

COMMANDER  
BMD SYSTEM COMMAND  
PO BOX 1500  
HUNTSVILLE, AL 35807  
ATTN BDMSC, TEN, NOAH J. HURST

COMMANDER  
FRANKFORD ARSENAL  
BRIDGE AND TACONY STREETS  
PHILADELPHIA, PA 19137  
ATTN SARFA-FCD, MARVIN ELNICK

COMMANDER  
PICATINNY ARSENAL  
DOVER, NJ 07801  
ATTN SARFA-ND-W  
ATTN SARFA-TN, BURTON V. FRANKS  
ATTN SARFA-ND-N  
ATTN SARFA-ND-N-E  
ATTN SARFA-FR-E, LOUIS AVRAMI

COMMANDER  
REDSTONE SCIENTIFIC INFORMATION CTR  
US ARMY MISSILE COMMAND  
REDSTONE ARSENAL, AL 35809  
ATTN CHIEF, DOCUMENTS

SECRETARY OF THE ARMY  
WASHINGTON, DC 20310  
ATTN ODUSA OR, DANIEL WILLIARD

COMMANDER  
TRASANA  
WHITE SANDS MISSILE RANGE, NM 88002  
ATTN ATAA-EAC, FRANCIS N. WINANS

DIRECTOR  
US ARMY BALLISTIC RESEARCH LABORATORIES  
ABERDEEN PROVING GROUND, MD 21005  
ATTN DRXBR-AM, W. R. VANANTWERP  
ATTN DRXBD-BVL, DAVID L. RIGOTTI  
ATTN DRXBR-X, JULIUS J. MESZAROS

COMMANDER  
US ARMY COMMUNICATIONS SYSTEMS AGENCY  
FORT MONMOUTH, NJ 07703  
ATTN SCCM-AD-SV (LIBRARY)

COMMANDER  
US ARMY ELECTRONICS COMMAND  
FORT MONMOUTH, NJ 07703  
ATTN DRSEL-CT-HDK, ABRAHAM E. COHEN  
ATTN DRSEL-TL-MD, GERHART K. GAULE  
ATTN DRSEL-TL-EN, ROBERT LUX  
ATTN DRSEL-GG-TD, W. R. WERK  
ATTN DRSEL-PL-ENV, HANS A. BOMKE  
ATTN DRSEL-TL-ND, S. KRONENBEY  
ATTN DRSEL-TL-IR, EDWIN T. HUNTER

COMMANDER-IN-CHIEF  
US ARMY EUROPE AND SEVENTH ARMY  
APO NEW YORK 09403  
ATTN ODCSE-E, AEAGE-PI

COMMANDER  
US ARMY MISSILE COMMAND  
REDSTONE ARSENAL, AL 35809  
ATTN DRCPM-PE-EA, WALLACE C. WAGNER  
ATTN DRSMI-RGD, VICTOR W. RUWE  
ATTN DRSMI-RRR, FAISON P. GIBSON  
ATTN DRCPM-MLTI, SPT JOE A SIMS  
ATTN DRSMI-RGI, HUGH GREEN  
ATTN DRCPM-LCEX, HOWARD H. HENRIKSEN

COMMANDER  
US ARMY MOBILITY EQUIP R&D CTR  
FORT BELVOIR, VA 22060  
ATTN STSFB-MW, JOHN W. BOND, JR.

CHIEF  
US ARMY NUC AND CHEMICAL SURETY GP  
BLDG, 2073, NORTH AREA  
FT. BELVOIR, VA 22060  
ATTN MOSG-ND, MAJ SIDNEY W. WINSLOW

COMMANDER  
US ARMY NUCLEAR AGENCY  
FORT BLISS, TX 79916  
ATTN ATCN-W, LTC LEONARD A. SLUGA

COMMANDER  
US ARMY RESEARCH OFFICE  
PO BOX 12211  
RESEARCH TRIANGLE PARK, NC 27709  
ATTN R. LONTZ

COMMANDER  
US ARMY TEST AND EVALUATION COMMAND  
ABERDEEN PROVING GROUND, MD 21005  
ATTN DRSTE-EL, F. I. KOLCHIN  
ATTN DRSTE-NB, R. P. GALASSO

CHIEF OF NAVAL RESEARCH  
NAVY DEPARTMENT  
ARLINGTON, VA 22217  
ATTN CODE 421, DORIS W. FADGETT  
ATTN CODE 427

COMMANDER  
NAVAL ELECTRONIC SYSTEMS COMMAND  
HEADQUARTERS  
WASHINGTON, DC 20360  
ATTN PME 117-21  
ATTN ELEX 05323, CLEVELAND F. WATKINS  
ATTN CODE 504510

DISTRIBUTION (Cont'd)

COMMANDING OFFICER  
NAVAL INTELLIGENCE SUPPORT CENTER  
4301 SUITLAND ROAD, BLDG 5  
WASHINGTON, DC 20390  
ATTN F. ALEXANDER

DIRECTOR  
NAVAL RESEARCH LABORATORY  
WASHINGTON, DC 20375  
ATTN CODE 6631, JAMES C. RITTER  
ATTN CODE 4004, EMANUEL L. BRANCATO  
ATTN CODE 2627, DORIS R. POLEN  
ATTN CODE 7701, JACK D. BROWN  
ATTN CODE 5216, HAROLD L. HUGHES  
ATTN CODE 5210, JOHN E. DAVEY  
ATTN CODE 601, E. WOLICKI

COMMANDER  
NAVAL SEA SYSTEMS COMMAND  
NAVY DEPARTMENT  
WASHINGTON, DC 20362  
ATTN SEA-9931, RILEY B. LANE  
ATTN SEA-9931, SAMUEL A. BARHAM

COMMANDER  
NAVAL SHIP ENGINEERING CENTER  
CENTER BUILDING  
HYATTSVILLE, MD 20782  
ATTN CODE 6174D2, EDWARD F. DUFFY

COMMANDER  
NAVAL SURFACE WEAPONS CENTER  
WHITE OAK, SILVER SPRING, MD 20910  
ATTN CODE WA501, NAVY NUC PRGMS OFF  
ATTN CODE WA50, JOHN H. MALLOY

COMMANDER  
NAVAL SURFACE WEAPONS CENTER  
DAHLGREN LABORATORY  
DAHLGREN, VA 22448  
ATTN WILLIAM H. HOLT

COMMANDER  
NAVAL WEAPONS CENTER  
CHINA LAKE, CA 93555  
ATTN CODE 533, TECHNICAL LIBRARY

COMMANDING OFFICER  
NAVAL WEAPONS SUPPORT CENTER  
CRANE, IN 47522  
ATTN CODE 70242, JOSEPH A. MUNARIN  
ATTN CODE 7024, JAMES RAMSEY

COMMANDING OFFICER  
NUCLEAR WEAPONS TRAINING CENTER PACIFIC  
NAVAL AIR STATION, NORTH ISLAND  
SAN DIEGO, CA 92135  
ATTN CODE 50

DIRECTOR  
STRATEGIC SYSTEMS PROJECT OFFICE  
NAVY DEPARTMENT  
WASHINGTON, DC 20376  
ATTN NSP-2342, RICHARD L. COLEMAN

GEOPHYSICS LABORATORY  
HANSCOM AFB, MA 01731  
ATTN J. EMERY CORMIER  
ATTN LQR, EDWARD A. BURKE

AF INSTITUTE OF TECHNOLOGY, AU  
WRIGHT-PATTERSON AFB, OH 45433  
ATTN ENP, CHARLES J. BRIDGMAN

AF MATERIALS LABORATORY, AFSC  
WRIGHT-PATTERSON AFB, OH 45433  
ATTN LTE

AF WEAPONS LABORATORY, AFSC  
KIRTLAND AFB, NM 87117  
ATTN SAT  
ATTN ELA  
ATTN SAB

AFTAC  
PATRICK AFB, FL 32925  
ATTN TAE

HEADQUARTERS  
ELECTRONIC SYSTEMS DIVISION, (AFSC)  
L. G. HANSCOM FIELD  
BEDFORD, MA 01730  
ATTN YSEV, LTC DAVID C. SPARKS

COMMANDER  
FOREIGN TECHNOLOGY DIVISION, AFSC  
WRIGHT-PATTERSON AFB, OH 45433  
ATTN ETET, CAPT RICHARD C. HUSEMANN

SAMSO/DY  
POST OFFICE BOX 92960  
WORLDWAY POSTAL CENTER  
LOS ANGELES, CA 90009  
ATTN DYS, CAPT WAYNE SCHOBER  
ATTN DYS, MAJ LARRY A. DARDA

SAMSO/IN  
POST OFFICE BOX 92960  
WORLDWAY POSTAL CENTER  
LOS ANGELES, CA 90009  
ATTN IND, T. J. JULY

SAMSO/MN  
NORTON AFB, CA 92409  
ATTN MNNG, CAPT DAVID J. STROBEL

SAMSO/RS  
POST OFFICE BOX 92960  
WORLDWAY POSTAL CENTER  
LOS ANGELES, CA 90009  
ATTN RSE  
ATTN RSSE, LTC KENNETH L. GILBERT

SAMSO/SZ  
POST OFFICE BOX 92960  
WORLDWAY POSTAL CENTER  
LOS ANGELES, CA 90009  
ATTN SZJ, CAPT JOHN H. SALCH

SAMSO/YD  
POST OFFICE BOX 92960  
WORLDWAY POSTAL CENTER  
LOS ANGELES, CA 90009  
ATTN YDD, MAJ M. F. SCHNEIDER

COMMANDER IN CHIEF  
STRATEGIC AIR COMMAND  
OFFUTT AFB, NE 68113  
ATTN NRI-STINFO LIBRARY  
ATTN XFFS, MAJ BRIAN STEPHAN

LOS ALAMOS SCIENTIFIC LABORATORY  
P.O. BOX 1663  
LOS ALAMOS, NM 87544  
ATTN MARVIN M. HOFFMAN  
ATTN J. ARTHUR FREED  
ATTN BRUCE W. NOEL

SANDIA LABORATORIES  
LIVERMORE LABORATORY  
PO BOX 969  
LIVERMORE, CA 94550  
ATTN THEODORE A. DELLIN  
ATTN P. L. MATTERN

SANDIA LABORATORIES  
PO BOX 5800  
ALBUQUERQUE, NM 87115  
ATTN 3141 SANDIA RPT COLL  
ATTN ORG 2110, J. A. HOOD  
ATTN ORG 1933, F. N. COPPAGE  
ATTN JACK V. WALKER, 5220  
ATTN R. C. HUGHES  
ATTN HOWARD SANDER  
ATTN DIV 5231, JAMES H. BENKEN

US ENERGY RSCH & DEV ADMIN  
ALBUQUERQUE OPERATIONS OFFICE  
PO BOX 5400  
ALBUQUERQUE, NM 87115  
ATTN WSSB

UNIVERSITY OF CALIFORNIA  
LAWRENCE LIVERMORE LABORATORY  
PO BOX 808  
LIVERMORE, CA 94550  
ATTN DONALD J. MEEKER, L-545  
ATTN HANS KRUGER, L-96  
ATTN TECH INFO DEPT, L-3  
ATTN LAWRENCE CLELAND, L-156  
ATTN RONALD L. OTT, L-531  
ATTN JOSEPH E. KELLER, JR., L-125  
ATTN FREDERICK R. KOVAR, L-31

CENTRAL INTELLIGENCE AGENCY  
ATTN RD/SI, RM 5648, HQ BLDG  
WASHINGTON, DC 20505  
ATTN ALICE A. PADGETT

DEPARTMENT OF COMMERCE  
NATIONAL BUREAU OF STANDARDS  
WASHINGTON, DC 20234  
ATTN JUDSON C. FRENCH  
ATTN APPL RAD DIV  
ROBERT C. PLACIUS  
ATTN SEMICONDUCTOR TECHNOLOGY,  
W. M. BULLIS  
ATTN K. F. GALLAWAY

AEROJET ELECTRO-SYSTEMS CO DIV  
AEROJET-GENERAL CORPORATION  
PO BOX 296  
AZUSA, CA 91702  
ATTN THOMAS D. HANSCOME

AERONUTRONIC FORD CORPORATION  
AEROSPACE & COMMUNICATIONS OPS  
AERONUTRONIC DIVISION  
FORD & JAMBOREE ROADS  
NEWPORT BEACH, CA 92663  
ATTN KEN C. ATTINGER  
ATTN TECH INFO SECTION

DISTRIBUTION (Cont'd)

AERONUTRONIC FORD CORPORATION  
WESTERN DEVELOPMENT LABORATORIES DIV  
3939 FABIAN WAY  
PALO ALTO, CA 94303  
ATTN SAMUEL R. CRAWFORD, MS 531  
ATTN DONALD R. MCMORROW, MS C30

AEROSPACE CORPORATION  
PO BOX 92957  
LOS ANGELES, CA 90009  
ATTN IRVING M. GARFUNKEL  
ATTN JULIAN REINHIMER  
ATTN LIBRARY  
ATTN MELVIN J. BERNSTEIN  
ATTN WILLIAM W. WILLIS  
ATTN L. W. AUKERMAN

AVCO RESEARCH & SYSTEMS GROUP  
201 LOWELL STREET  
WILMINGTON, MA 01887  
ATTN RESEARCH LIBRARY, A830, RM 7201

BDM CORPORATION, THE  
PO BOX 9274  
ALBUQUERQUE INTERNATIONAL  
ALBUQUERQUE, NM 87119  
ATTN T. H. NEIGHBORS

BENDIX CORPORATION, THE  
COMMUNICATION DIVISION  
EAST JOPPA ROAD - TOWSON  
BALTIMORE, MD 21204  
ATTN DOCUMENT CONTROL

BENDIX CORPORATION, THE  
RESEARCH LABORATORIES DIV  
BENDIX CENTER  
SOUTHFIELD, MI 48075  
ATTN MGR PRGM DEV,  
DONALD J. NIEHAUS

BOEING COMPANY, THE  
PO BOX 3707  
SEATTLE, WA 98124  
ATTN HOWARD W. WICKLEIN, MS 17-11  
ATTN DAVID DYE, MS 87-75  
ATTN AEROSPACE LIBRARY  
ATTN ROBERT S. CALDWELL, 2R-00

BOOZ-ALLEN AND HAMILTON, INC.  
106 APPLE STREET  
NEW SHREWSBURY, NJ 07724  
ATTN R. J. CHRISNER

CALIFORNIA INSTITUTE OF TECHNOLOGY  
JET PROPULSION LABORATORY  
4800 OAK GROVE  
PASADENA, CA 91103  
ATTN A. G. STANLEY  
ATTN J. BRYDEN

CHARLES STARK DRAPER LABORATORY INC.  
68 ALBANY STREET  
CAMBRIDGE, MA 02139  
ATTN KENNETH FERTIG  
ATTN RICHARD G. HALTMAIER  
ATTN PAUL R. KELLY

COMPUTER SCIENCES CORPORATION  
201 LA VETA DRIVE, NE  
ALBUQUERQUE, NM 87108  
ATTN RICHARD H. DICKHAUT

C. T. SAH ASSOCIATES  
PO BOX 364  
URBANA, IL 61801  
ATTN C. T. SAH

CUTLER-HAMMER, INC.  
AIL DIVISION  
COMAC ROAD  
DEER PARK, NY 11729  
ATTN CENTRAL TECH FILES,  
ANN ANTHONY

DIKEWOOD CORPORATION, THE  
1009 BRADBURY DRIVE, SE  
UNIVERSITY RESEARCH PARK  
ALBUQUERQUE, NM 87106  
ATTN L. WAYNE DAVIS

E-SYSTEMS, INC.  
GREENVILLE DIVISION  
PO BOX 1056  
GREENVILLE, TX 75401  
ATTN LIBRARY 8-50100

EFFECTS TECHNOLOGY, INC.  
5383 HOLISTER AVENUE  
SANTA BARBARA, CA 93105  
ATTN EDWARD JOHN STEELE

ELECTRONICS TECHNOLOGY LABORATORY  
ENGINEERING EXPERIMENT STATION  
GEORGIA INSTITUTE OF TECHNOLOGY  
ATLANTA, GA 30332  
ATTN R. CURRY

EXPERIMENTAL AND MATHEMATICAL  
PHYSICS CONSULTANTS  
P. O. BOX 66331  
LOS ANGELES, CA 90066  
ATTN THOMAS M. JORDAN

FAIRCHILD CAMERA AND  
INSTRUMENT CORPORATION  
464 ELLIS STREET  
MOUNTAIN VIEW, CA 94040  
ATTN 2-233, MR. DAVID K. MYERS

FAIRCHILD INDUSTRIES, INC.  
SHERMAN FAIRCHILD TECHNOLOGY CENTER  
20301 CENTURY BOULEVARD  
GERMANTOWN, MD 20767  
ATTN MGR CONFIG DATA & STANDARDS

UNIVERSITY OF FLORIDA  
231 AEROSPACE BLDG  
GAINESVILLE, FL 32611  
ATTN D. P. KENNEDY

FRANKLIN INSTITUTE, THE  
20TH STREET AND PARKWAY  
PHILADELPHIA, PA 19103  
ATTN FAMIE H. THOMPSON

GENERAL DYNAMICS CORP  
ELECTRONICS DIV ORLANDO OPERATIONS  
PO BOX 2566  
ORLANDO, FL 32802  
ATTN D. W. COLEMAN

GENERAL ELECTRIC COMPANY  
SPACE DIVISION  
VALLEY FORGE SPACE CENTER  
P.O. BOX 8555  
PHILADELPHIA, PA 19101  
ATTN JAMES P. SPRATT  
ATTN LARRY I. CHASEN  
ATTN JOSEPH C. PEDEN, CCF 8301  
ATTN JOHN L. ANDREWS  
ATTN CSP 6-7, RICHARD C. FRIES

GENERAL ELECTRIC COMPANY  
RE-ENTRY & ENVIRONMENTAL SYSTEMS DIV  
PO BOX 7722  
3198 CHESTNUT STREET  
PHILADELPHIA, PA 19101  
ATTN ROBERT V. BENEDICT

GENERAL ELECTRIC COMPANY  
ORDNANCE SYSTEMS  
100 PLASTICS AVENUE  
PITTSFIELD, MA 01201  
ATTN JOSEPH J. REIDL

GENERAL ELECTRIC COMPANY  
TEMPO-CENTER FOR ADVANCED STUDIES  
816 STATE STREET (PO DRAWER QQ)  
SANTA BARBARA, CA 93102

ATTN DASIAC  
ATTN ROYDEN R. RUTHERFORD  
ATTN M ESPIG

GENERAL ELECTRIC COMPANY  
PO BOX 1122  
SYRACUSE, NY 13201  
ATTN CSP 6-7, RICHARD C. FRIES  
ATTN CSP 0-7, L. H. DEE

GENERAL ELECTRIC COMPANY  
AIRCRAFT ENGINE GROUP  
EVENDALE PLANT  
CINCINNATI, OH 45215  
ATTN JOHN A. ELLERHORST, E2

GENERAL ELECTRIC COMPANY  
AEROSPACE ELECTRONICS SYSTEMS  
FRENCH ROAD  
UTICA, NY 13503  
ATTN W. J. PATTERSON, DROP 233

GENERAL ELECTRIC COMPANY  
PO BOX 5000  
BINGHAMTON, NY 13902  
ATTN DAVID W. PEPIN, DROP 160

GENERAL ELECTRIC COMPANY-TEMPO  
ATTN: DASIAC  
C/O DEFENSE NUCLEAR AGENCY  
WASHINGTON, DC 20305  
ATTN WILLIAM ALFONTE

DISTRIBUTION (Cont'd)

GENERAL RESEARCH CORPORATION  
P.O. BOX 3587  
SANTA BARBARA, CA 93105  
ATTN ROBERT D. HILL

GRUMMAN AEROSPACE CORPORATION  
SOUTH OYSTER BAY ROAD  
BETHPAGE, NY 11714  
ATTN JERRY ROGERS, DEPT 533

GTE SYLVANIA, INC.  
ELECTRONICS SYSTEMS GRP-EASTERN DIV  
77 A STREET  
NEEDHAM, MA 02194  
ATTN CHARLES A. THORNHILL, LIBRARIAN  
ATTN LEONARD L. BLAISDELL  
ATTN JAMES A. WALDON

GTE SYLVANIA, INC.  
189 B STREET  
NEEDHAM HEIGHTS, MA 02194  
ATTN CHARLES H. RAMSBOTTOM  
ATTN HERBERT A. ULLMAN  
ATTN H & V GROUP, MARIO A. NUREFORA  
ATTN PAUL B. FREDRICKSON

HARRIS CORPORATION  
HARRIS SEMICONDUCTOR DIVISION  
P.O. BOX 583  
MELBOURNE, FL 32901  
ATTN C. F. DAVIS, MS 17-220  
ATTN T. CLARK, MS 4040  
ATTN WAYNE E. ABARE, MS 16-111

HAZELTINE CORPORATION  
PULASKI ROAD  
GREEN LAWN, NY 11740  
ATTN TECH INFO CTR, M. WAITE

HONEYWELL INCORPORATED  
GOVERNMENT AND AERONAUTICAL  
PRODUCTS DIVISION  
2600 RIDGEWAY PARKWAY  
MINNEAPOLIS, MN 55413  
ATTN RONALD R. JOHNSON, A1622

HONEYWELL INCORPORATED  
AEROSPACE DIVISION  
13350 US HIGHWAY 19  
ST. PETERSBURG, FL 33733  
ATTN MS 725-J, STACEY H. GRAFF

HONEYWELL INCORPORATED  
RADIATION CENTER  
2 FORBES ROAD  
LEXINGTON, MA 02173  
ATTN TECHNICAL LIBRARY

HUGHES AIRCRAFT COMPANY  
CENTINELA & TEALF  
CULVER CITY, CA 90230  
ATTN M.S. D157, KEN WALKER  
ATTN B. W. CAMPBELL, M.S. 6-E110  
ATTN DAN BINDER, MS 6-D147

HUGHES AIRCRAFT COMPANY  
SPACE SYSTEMS DIVISION  
P.O. BOX 92919  
LOS ANGELES, CA 90009  
ATTN WILLIAM W. SCOTT, MS A1080  
ATTN EDWARD C. SMITH, MS A620

HUGHES AIRCRAFT COMPANY  
500 SUPERIOR AVE  
NEWPORT BEACH, CA 92663  
ATTN KENNETH AUBUCHON  
ATTN ELI HARARI

IBM CORPORATION  
ROUTE 17C  
OWEGO, NY 13827  
ATTN FRANK FRANKOVSKY

INTELCOM RAD TECH  
P.O. BOX 81087  
SAN DIEGO, CA 92138  
ATTN ROLAND LEADON  
ATTN T. M. FLANAGAN

ION PHYSICS CORPORATION  
SOUTH BEDFORD STREET  
BURLINGTON, MA 01803  
ATTN ROBERT D. EVANS

IRT CORPORATION  
PO BOX 81087  
SAN DIEGO, CA 92138  
ATTN MDC  
ATTN JAMES A. NABER  
ATTN RALPH H. STAHL  
ATTN R. L. MERTZ

KAMAN SCIENCES CORPORATION  
P.O. BOX 7463  
COLORADO SPRINGS, CO 80933  
ATTN DONALD H. BRYCE  
ATTN ALBERT P. BRIDGES  
ATTN WALTER E. WARE

LEHIGH UNIVERSITY  
MATERIALS RESEARCH CENTER  
BETHLEHEM, PA 18015  
ATTN S. R. BUTLER  
ATTN F. J. FEIGL  
ATTN F. M. FOWKES

LITTON SYSTEMS, INC.  
GUIDANCE & CONTROL SYSTEMS DIVISION  
5500 CANOGA AVENUE  
WOODLAND HILLS, CA 91364  
ATTN VAL J. ASHBY, MS 67  
ATTN JOHN P. RETZLER

LOCKHEED MISSILES AND SPACE  
COMPANY, INC.  
P.O. BOX 504  
SUNNYVALE, CA 94088  
ATTN G. F. HEATH, D/81-14  
ATTN BENJAMIN T. KIMURA,  
DEPT 81-14, BLDG 154  
ATTN EDWIN A. SMITH, DEPT 85-85  
ATTN PHILIP J. HART, DEPT 81-14  
ATTN L. ROSSI, DEPT 81-64  
ATTN DEPT 81-01, G. H. MORRIS

LOCKHEED MISSILES AND SPACE COMPANY  
3251 HANOVER STREET  
PALO ALTO, CA 94304  
ATTN TECH INFO CTR D/COLL

LTV AEROSPACE CORPORATION  
VOUGHT SYSTEMS DIVISION  
P.O. BOX 6267  
DALLAS, TX 75222  
ATTN TECHNICAL DATA CENTER

LTV AEROSPACE CORPORATION  
PO BOX 5907  
DALLAS, TX 75222  
ATTN TECHNICAL DATA CTR

M.I.T. LINCOLN LABORATORY  
P.O. BOX 73  
LEXINGTON, MA 02173  
ATTN LEONA LOUGHLIN, LIBRARIAN A-062

MARTIN MARIETTA AEROSPACE  
ORLANDO DIVISION  
P.O. BOX 5837  
ORLANDO, FL 32805  
ATTN MONA C. GRIFFITH, LIB MF-30  
ATTN WILLIAM W. MEAS, MP-413

MARTIN MARIETTA CORPORATION  
DENVER DIVISION  
PO BOX 179  
DENVER, CO 80201  
ATTN J. E. GOODWIN, MAIL 0452  
ATTN RESEARCH LIB, 6617, J. R. MCKEE  
ATTN BEN T. CRAHAM, MS PO-454

MCDONNELL DOUGLAS CORPORATION  
POST OFFICE BOX 516  
ST. LOUIS, MO 63166  
ATTN TECHNICAL LIBRARY

MCDONNELL DOUGLAS CORPORATION  
5301 BOLSA AVENUE  
HUNTINGTON BEACH, CA 92647  
ATTN STANLEY SCHNEIDER

MISSION RESEARCH CORPORATION  
735 STATE STREET  
SANTA BARBARA, CA 93101  
ATTN WILLIAM C. HART

MISSION RESEARCH CORPORATION-SAN DIEGO  
7650 CONVOY COURT  
SAN DIEGO, CA 92111  
ATTN V. A. J. VAN LINT

NATIONAL ACADEMY OF SCIENCES  
2101 CONSTITUTION AVE, NW  
WASHINGTON, DC 20418  
ATTN DR. R. S. SHANE,  
NAT MATERIALS ADVISORY BOARD

UNIVERSITY OF NEW MEXICO  
DEPT OF CAMPUS SECURITY AND POLICE  
1821 ROMA NE  
ALBUQUERQUE, NM 87106  
ATTN W. W. GRANNEMANN

NORTHROP CORPORATION  
ELECTRONIC DIVISION  
1 RESEARCH PARK  
PALOS VERDES PENINSULA, CA 90274  
ATTN VINCENT R. DEMARTINO  
ATTN BOYCE T. AHLFORT  
ATTN GEORGE H. TOWNER

NORTHROP CORPORATION  
NORTHROP RESEARCH AND TECHNOLOGY CENTER  
3401 WEST BROADWAY  
HAWTHORNE, CA 90250  
ATTN DAVID N. POCOCC  
ATTN JOSEPH R. SHOUR

DISTRIBUTION (Cont'd)

PHYSICS INTERNATIONAL COMPANY  
2700 MERCED STREET  
SAN LEANDRO, CA 94577  
ATTN CHARLES H. STALLINGS  
ATTN JOHN H. HUNTINGTON

PRINCETON UNIVERSITY  
DEPT OF AEROSPACE &  
MECHANICAL SCIENCES  
PRINCETON, NJ 08940  
ATTN BARRIE S. H. ROYCE

R & D ASSOCIATES  
PO BOX 9695  
MARINA DEL REY, CA 90291  
ATTN S. CLAY ROGERS

RAYTHEON COMPANY  
HARTWELL ROAD  
BEDFORD, MA 01730  
ATTN GAJANAN H. JOSHI,  
RADAR SYS LAB

RCA CORPORATION  
GOVERNMENT & COMMERCIAL SYSTEMS  
ASTRO ELECTRONICS DIVISION  
PO BOX 800, LOCUST CORNER  
PRINCETON, NJ 08540  
ATTN GEORGE J. BRUCKER

RCA CORPORATION  
DAVID SARNOFF RESEARCH CENTER  
W. WINDSOR TWP  
201 WASHINGTON ROAD, PO BOX 432  
PRINCETON, NJ 08540  
ATTN K. H. ZAININGER  
ATTN R. J. POWELL

RENSELAER POLYTECHNIC INSTITUTE  
PO BOX 965  
TROY, NY 12181  
ATTN RONALD J. GUTMANN

RESEARCH TRIANGLE INSTITUTE  
PO BOX 12194  
RESEARCH TRIANGLE PARK, NC 27709  
ATTN ENG DIV, MAYRANT SIMONS, JR.

ROCKWELL INTERNATIONAL CORPORATION  
3370 MIRALOMA AVENUE  
ANAHEIM, CA 92803  
ATTN K. F. HULL  
ATTN JAMES E. BELL, HA10  
ATTN DONALD J. STEVENS, FA70  
ATTN GEORGE C. MESSENGER, FB61

ROCKWELL INTERNATIONAL CORPORATION  
ELECTRONICS OPERATIONS  
COLLINS RADIO GROUP  
5225 C. AVE NE  
CEDAR RAPIDS, IA 52406  
ATTN DENNIS SUTHERLAND

SANDERS ASSOCIATES, INC.  
95 CANAL STREET  
NASHUA, NH 03060  
ATTN M. L. AITEL, NCA 1-3236

SCIENCE APPLICATIONS, INC.  
1651 OLD MEADOW ROAD  
MCLEAN, VA 22101  
ATTN WILLIAM L. CHADSEY

SCIENCE APPLICATIONS, INC.  
PO BOX 2351  
LA JOLLA, CA 92038  
ATTN LARRY SCOTT  
ATTN J. ROBERT BEYSTER

SCIENCE APPLICATIONS, INC.  
HUNTSVILLE DIVISION  
2109 W. CLINTON AVENUE  
SUITE 700  
HUNTSVILLE, AL 35805  
ATTN NOEL R. BYRN

SCIENCE APPLICATIONS, INC.  
2680 HANOVER STREET  
PALO ALTO, CA 94303  
ATTN CHARLES STEVENS

SIMULATION PHYSICS, INC.  
41 "B" STREET  
BURLINGTON, MA 01803  
ATTN ROGER G. LITTLE

SINGER COMPANY, THE  
1150 MC BRIDE AVENUE  
LITTLE FALLS, NJ 07424  
ATTN IRWIN GOLDMAN, ENG MANAGEMENT

SINGER COMPANY (DATA SYSTEMS), THE  
150 TOTOWA ROAD  
WAYNE, NJ 07470  
ATTN TECH INFO CENTER

SPERRY RAND CORPORATION  
SPERRY DIVISION  
SPERRY GYROSCOPE DIVISION  
SPERRY MANAGEMENT DIVISION  
MARCUS AVENUE  
GREAT NECK, NY 11020  
ATTN PAUL MARRAFFINO  
ATTN CHARLES L. CRAIG EV

STANFORD RESEARCH INSTITUTE  
333 RAVENSWOOD AVENUE  
MENLOW PARK, CA 94025  
ATTN MR. PHILIP DOLAN  
ATTN ROBERT A. ARMISTEAD

STANFORD RESEARCH INSTITUTE  
306 WYNN DRIVE, N. W.  
HUNTSVILLE, AL 35805  
ATTN MACPHERSON MORGAN

SUNDSTRAND CORPORATION  
4751 HARRISON AVENUE  
ROCKFORD, IL 61101  
ATTN DEPT 763SW, CURTIS WHITE

TEXAS INSTRUMENTS, INC.  
P.O. BOX 5474  
DALLAS, TX 75222  
ATTN DONALD J. MANUS, MS 72

TRW SYSTEMS GROUP  
ONE SPACE PARK  
REDONDO BEACH, CA 90278  
ATTN R. D. LOVELAND, R1-1028  
ATTN A. A. WITTELES, MS R1-1120  
ATTN TECH INFO CENTER/S-1930  
ATTN A. M. LIEBSCHUTZ R1-1162  
ATTN AARON H. NAREVSKY, R1-2144  
ATTN RICHARD H. KINGSLAND, R1-2154  
ATTN JERRY I. LUBELL  
ATTN LILLIAN D. SINGLETARY, R1/1070  
ATTN WILLIAM H. ROBINETTE, JR.  
ATTN PAUL MOLMUD, R1-1196  
ATTN ALLAN ANDERMAN, R1-1132

TRW SYSTEMS GROUP  
SAN BERNARDINO OPERATIONS  
PO BOX 1310  
SAN BERNARDINO, CA 92402  
ATTN EARL W. ALLEN  
ATTN JOHN E. DAHNKE  
ATTN H. S. JENSEN

WESTINGHOUSE ELECTRIC CORPORATION  
DEFENSE AND ELECTRONIC SYSTEMS CENTER  
P.O. BOX 1693  
FRIENDSHIP INTERNATIONAL AIRPORT  
BALTIMORE, MD 21203  
ATTN HENRY P. KALAPACA, MS 3525

WESTINGHOUSE ELECTRIC CORPORATION  
RESEARCH AND DEVELOPMENT CENTER  
1310 BEULAH ROAD, CHURCHILL BOROUGH  
PITTSBURGH, PA 15235  
ATTN WILLIAM E. NEWELL

COMMANDER  
HARRY DIAMOND LABORATORIES  
2800 POWDER MILL RD  
ADELPHI, MD 20783  
ATTN MCGREGOR, THOMAS, COL, COMMANDER

FLYER, I.N./LANDIS, F.F./  
SOMMER, H./OSWALD, E. P.  
ATTN CARTER, W.W., DR., TECHNICAL  
DIRECTOR/MARCUS, S.M.

ATTN KIMMEL, S., PAO  
ATTN CHIEF, 0021  
ATTN CHIEF, 0022  
ATTN CHIEF, LAB 100  
ATTN CHIEF, LAB 200  
ATTN CHIEF, LAB 300  
ATTN CHIEF, LAB 400  
ATTN CHIEF, LAB 500  
ATTN CHIEF, LAB 600  
ATTN CHIEF, DIV 700  
ATTN CHIEF, DIV 800  
ATTN CHIEF, LAB 900  
ATTN CHIEF, LAB 1000  
ATTN RECORD COPY, BR 041  
ATTN HDL LIBRARY (3 COPIES)  
ATTN CHAIRMAN, EDITORIAL COMMITTEE  
ATTN CHIEF, 047  
ATTN TECH REPORTS, 013  
ATTN PATENT LAW BRANCH, 071  
ATTN MCLAUGHLIN, F.W., 741  
ATTN LANHAM, C., 0021  
ATTN CHIEF, BR 230  
ATTN ROSADO, J. A., 240  
ATTN CHIEF, BR 280  
ATTN CALDWELL, P. A., 290  
ATTN SCHALLHORN, D. R., 230  
ATTN OLDHAM, T. R., 230  
ATTN SCHARF, W. D., 230  
ATTN BOESCH, H. E., JR. 260  
ATTN WINOKUR, P. S., 280  
ATTN WIMENITZ, F. N., 0024  
ATTN MCGARRITY, J. M., 280  
ATTN SOKOLOSKI, M. M., 0021 (20 COPIES)  
ATTN AUSMAN, G. A., 210  
ATTN MCLEAN, F. B., 280